MEASUREMENTS OF INSOLATION VARIATION OVER A SOLAR COLLECTOR FIELD

December 30, 1978

Work Performed Under Contract No. ET-78-C-03-2028

Laboratory Operations
The Aerospace Corporation
El Segundo, California

U.S. Department of Energy

Solar Energy

NOTICE

ATR-79(7747)-2
Distribution Category UC-62d

MEASUREMENTS OF INSOLATION VARIATION OVER A SOLAR COLLECTOR FIELD

30 December 1978

Prepared By

Laboratory Operations
THE AEROSPACE CORPORATION
El Segundo, California 90245

Prepared for
U.S. Department of Energy

Contract ET-78-C-03-2028

PRINCIPAL CONTRIBUTORS

C. M. Randall, Chemistry and Physics Laboratory

M. E. Whitson, Jr., Chemistry and Physics Laboratory

B. R. Johnson, Chemistry and Physics Laboratory

ABSTRACT

The experiment described in this report makes observations to determine the direct insolation every 16 sec at corners of a quadrilateral approximately 600 meters in size located near Barstow, California. This size approximates the collector field of the solar power plant to be built near Barstow. Data from the first three months of operation of this experiment indicate cloudy conditions, capable of affecting the operation of a solar power plant, occurred during 15% of the daylight hours of some months. Patterns of insolation variation over the experiment area indicate shadows often exist with dimensions less than the projected size of the collection field for the 10 MW_e solar thermal power plant. Detailed statistical summaries of four partly cloudy events are included in this report.

Rates of insolation change on an individual sensor greater than ≥ 30 Wm^{-2} sec^{-1} have been observed, but these rate measurements have probably been limited by the response time of the experimental system. Spatial averaging of the measured insolation over the sensor field lowers the rate of insolation change.

ACKNOWLEDGMENTS

The rapidity with which the requirement for detailed experimental data on insolation variation was transformed into a working experiment deployed at Barstow is due to the dedicated cooperation of numerous people from several organizations. The authors of this report are deeply grateful for their individual contributions.

The Solar Ten Megawatt Project Office under the leadership of R. N. Schweinberg and Alex Klein has provided direction, funding and a forum for coordination of the experiment.

The Sandia Laboratories contributed instruments, a trailer to house the base station and cables to link the remote stations to the base station. These contributions were coordinated by John Otts.

The Southern California Edison Company provided the site, installed the basic facilities for the experiment and provides the routine maintenance. Lynn Rasband has coordinated the overall effort, with Bob Yinger providing detailed coordination, including site visits during set-up phases of the experiment. Foy Henry and Dan Whitney and others of the Coolwater Generating station at Daggett California, under the direction of Plant Engineer, C. L. Coss, and Supervisor of Instrumentation, Jon Davis, continue to provide the routine maintenance of the experiment.

Ed Flowers of The National Oceanic and Atmospheric Administration, Environmental Research Laboratories, provided the Normal Incidence Pyrheliometer calibrated against national standards which forms the basis of the calibration of the present experiment.

The personnel of the Federal Aviation Agency Flight Service Center at Daggett are supporting this experiment by supplying directly to us copies of the hourly surface weather observations from Daggett.

At Aerospace enthusiastic support and coordination has been provided by Energy Projects Directorate personnel H. Eden, T. Connor and J. Coggi under the leadership of E. L. Katz. Design and construction of all the specialized electronic circuitry required to assemble the experiment was directed by H. R. Hedgepeth of the Chemistry and Physics Laboratory. G. De Lao contributed significantly to all aspects of the experiment construction and deployment. The support of all these persons to the experiment described here is gratefully acknowledged.

CONTENTS

TABLES

FIGURES

I. INTRODUCTION

Rapid variations of insolation in both time and space have been identified as a potentially important concern in the design and operation the Solar 10 MW_e Pilot Plant presently planned for construction near Barstow, California. These rapid changes will affect the design of both the master plant control system and the individual receiver panel control systems (Ref. 1). The changes must also be accounted for in estimating the thermal fatigue in critical receiver elements.

A review of available data revealed little directly applicable information on variations during cloudy periods, but meteorological data indicate a significant portion of the daylight hours at Barstow have some cloud cover. Table 1-1 shows by months the mean fraction of daylight hours reported to have zero tenths cloud cover. The data examined cover the period 1946 through 1976 (Ref. 2).

Insolation data with satisfactory temporal and spatial resolution for transient studies are not available. The West Associates/SCE data from Barstow (Ref. 3, 4, 5) provide an excellent measure of the average energy available at the plant site, but they are 15-minute averages and involve only one instrument, thus giving no information about the spatial extent of the variations. A sample of the SCE data is shown in Fig. 1-1 for comparison with 15-minute averages of data obtained in the current study presented in Chapter III. Data with time resolution down to a minute are available from some locations, but in all cases they involve only one sensor and are not from the geographic area of interest. Helio Associates (Ref. 6) made a pioneering study of spatial variation over distances of 1-3 miles, but their instrumentation permitted a temporal resolution of best 3-6 minutes.

Table 1-1. Percent of Daylight Hours with Zero Total Sky Cover

(Source: 1948-1976 Daggett Hourly Surface Weather Observations)

MONTH	PERCENT CLEAR DAYLIGHT HOURS
JANUARY	35
FEBRUARY	39
MARCH	40
DECEMBER	40
APRIL	47
NOVEMBER	49
MAY	55
JULY	57
AUGUST	60
OCTOBER	61
SEPTEMBER	71
JUNE	73
ANNUAL	52

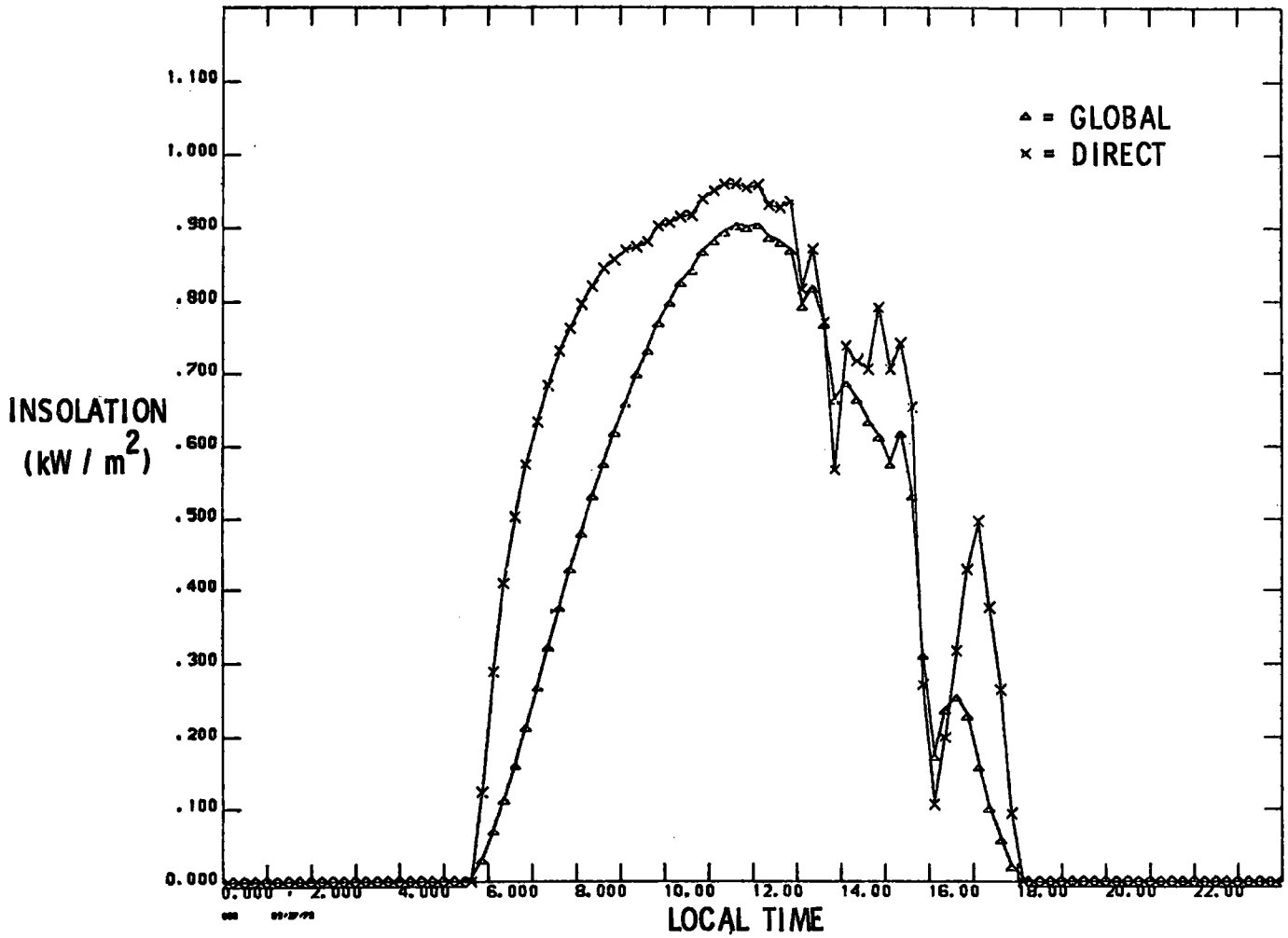

Figure 1-1. Fifteen Minute Averages of Insolation Observed on 1 April 1977 by the Southern California Edison Co. at Barstow California.

The use of cloud photographs appears initially to be an attractive approach for studying the insolation variation over the collector field. Indeed, in the absence of other data this was the approach used in the initial Aerospace efforts to model these effects (Ref. 7). These initial studies were based on photographs taken from high flying aircraft, and cloud-free line of sight analyses (Ref. 8, 9). More recent aircraft data (Ref. 10) were added to an extension of these studies which included detailed simulation of the effects on a solar collector array (Ref. 11). However, the basic approach and its limitations remained: a) the resolution of the photographs did not permit extension of the size distributions below about 1 km, and b) no temporal information was available, so that motion had to be estimated from separate "winds aloft" studies. Since no information was available about small clouds, the resulting model (Ref. 11) consisted of a semi-infinite shadow which could be moved at arbitrary speed and direction across the collector array. More recently, satellite data with resolution down to 0.6 km (DMSP) have become available, but only once per day and from SMS every 1/2 hour at a resolution of 0.9 km. Sample data from these satellites have recently been analysed (Ref. 12, 13) for cloud size distributions, confirming the distributions found by earlier workers, but the spatial resolution and lack of temporal resolution, as well as the time involved in the manual analysis technique precludes the direct application of satellite data to the design and performance analysis of the pilot plant.

Based on the need for these data and the unavailability of suitable data from other sources the Solar Ten Megawatt Project Office (STMPO) in the spring of 1978 asked Aerospace to make suitable measurements utilizing both Aerospace resources and those of other STMPO contractors to assure the availability of data at the earliest possible time. Chapter II of this report describes the experiment which was deployed in the field near Barstow some two months later on 3 August. The speed with which this was

accomplished is due to the cooperation of all the organizations listed in the acknowledgment section of this report. Chapter III presents the results of our initial analysis of data from the first 3 months of operation. Chapter IV is a summary of our present results and recommendations.

The experiment is continuing to accumulate data and may in the near future be improved somewhat. Therefore, the present document should be regarded as an interim report, particularly in the case of data analysis.

II. EXPERIMENT DESCRIPTION

A. INTRODUCTION

The purpose of the insolation variation experiment is to provide data describing the temporal and spatial variation of insolation in a form which can be used in the detailed design of the pilot plant. This section will describe the actual experiment deployed in the Barstow area.

The ideal experimental configuration for defining insolation variation over a field which will contain n focusing mirrors is obviously an array of n direct insolation measuring devices. Such a system cannot actually be produced owing to the cost of the equipment, data reduction, and maintenance. At the time this experiment was conceived, the number and spacing of sensors required to characterize insolation variation over a field having the dimensions of the pilot plant was unknown. Consideration of expense, time, and analysis factors, together with guesses based upon physical intuition, led to the choice of a 4-point square array of sensors. The dimensions of the array of pilot plant heliostats, approximately 600 m x 600 m, defined the spacing of the insolation sensors, and thus the spatial resolution of the experiment. The required temporal resolution actually would be defined by minimum pilot plant servo times, if these were known. Since such a parameter is not well defined and in fact may be chosen on the basis of the data obtained in this experiment, a system was constructed to measure 16 sec averages of insolation signals with the capability of simple modification to 4, 8 or 32 sec operation. To date, only 16 sec data have been acquired.

Measurement of direct insolation at all 4 data acquisition stations was judged to be undesirable, since this would substantially increase the equipment costs and periodic maintenance of the system. Direct insolation is measured using a normal incidence pyrheliometer (NIP) mounted on a solar tracker which must be adjusted for declination

every few days. It was concluded that adequate accuracy could be obtained from remote stations equipped with pyranometers measuring global insolation. These are static devices requiring only cleaning. With this configuration AC power is required at only one station and at that location a NIP, pyranometers, and a shadow band pyranometer are deployed in order to measure the quantities necessary for calculating direct insolation from the global measurements at the remote stations. A block diagram of the experiment, including the data acqusition system is provided in Fig. 2-1.

B. SITE

A suitable site large enough to allow full coverage of a 600 m x 600 m field was found at the Southern California Edison (SCE) Coolwater Generating Plant. The site is adjacent to the pilot plant location and within 2 miles of the Daggett airport, where meteorological data are recorded hourly by the Federal Aviation Agency (FAA). The relative locations of the SCE insolation measuring site in Barstow, the Daggett airport, and the pilot plant site are shown in Fig. 2-2. Figure 2-3 illustrates the instrument placement around the Coolwater Plant evaporation pond. The area is physically secure since it is surrounded by an 8 foot chain link fence, and it is a low traffic area for SCE employees.

An instrument trailer, is situated at the northwest corner of the pond and serves as the base station for the experiment. Power is provided at this location by SCE. At the 3 remote instrument stations, poles were set by SCE.

C. EQUIPMENT

At all 4 instrument stations, illustrated in Fig. 2-3, a Lambda LI-200S pyranometer is mounted. This device is a low-cost, reliable sensor. This sensor has been shown to compare favorably with Eppley PSP instruments costing about 8 times as much (Ref. 14). At the base station, station 4 of Fig. 2-3, a fifth Lambda pyranometer is

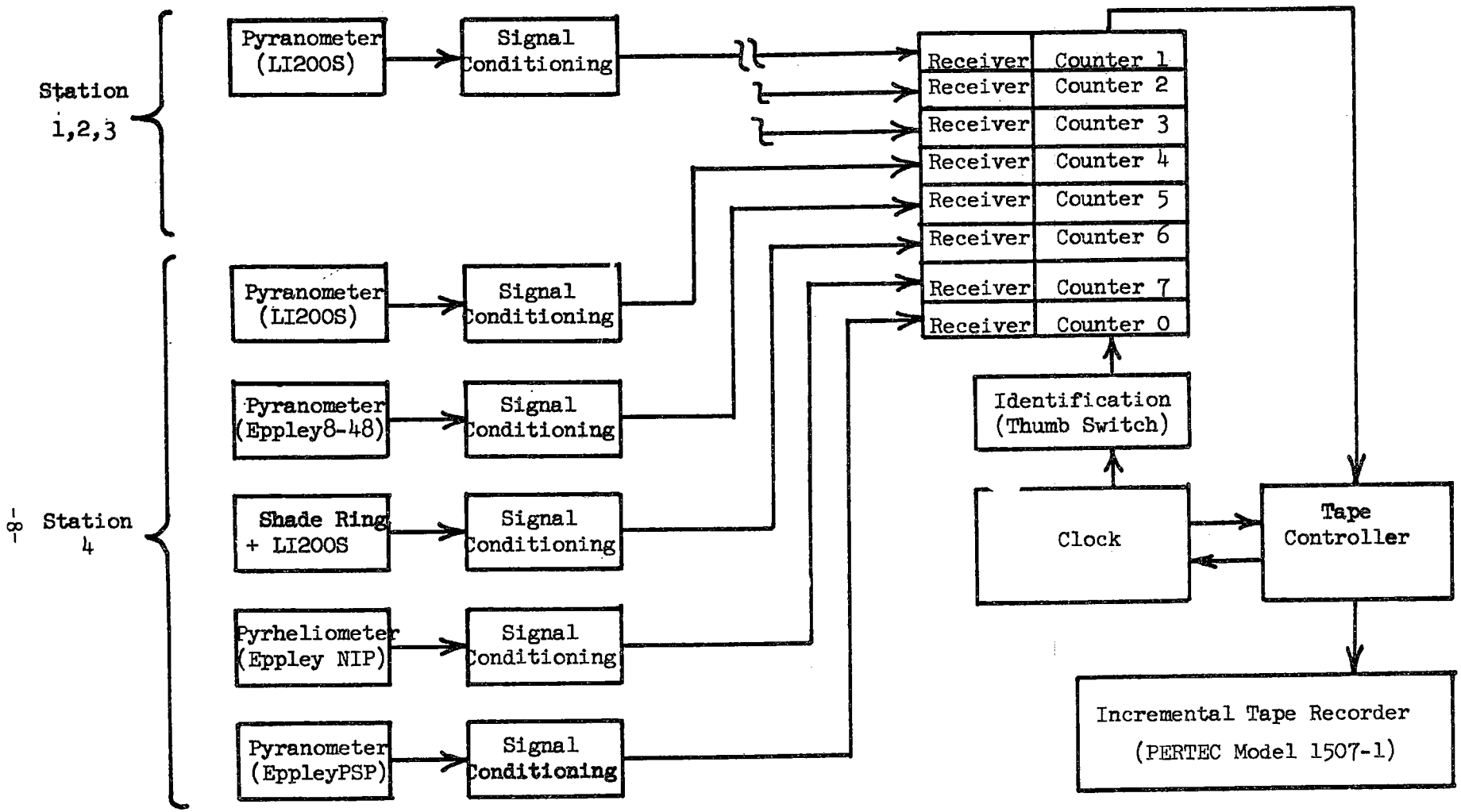

Figure 2-1. Block Diagram of the Insolation Variation Experiment.

Figure 2-2. **Barstow California Area**

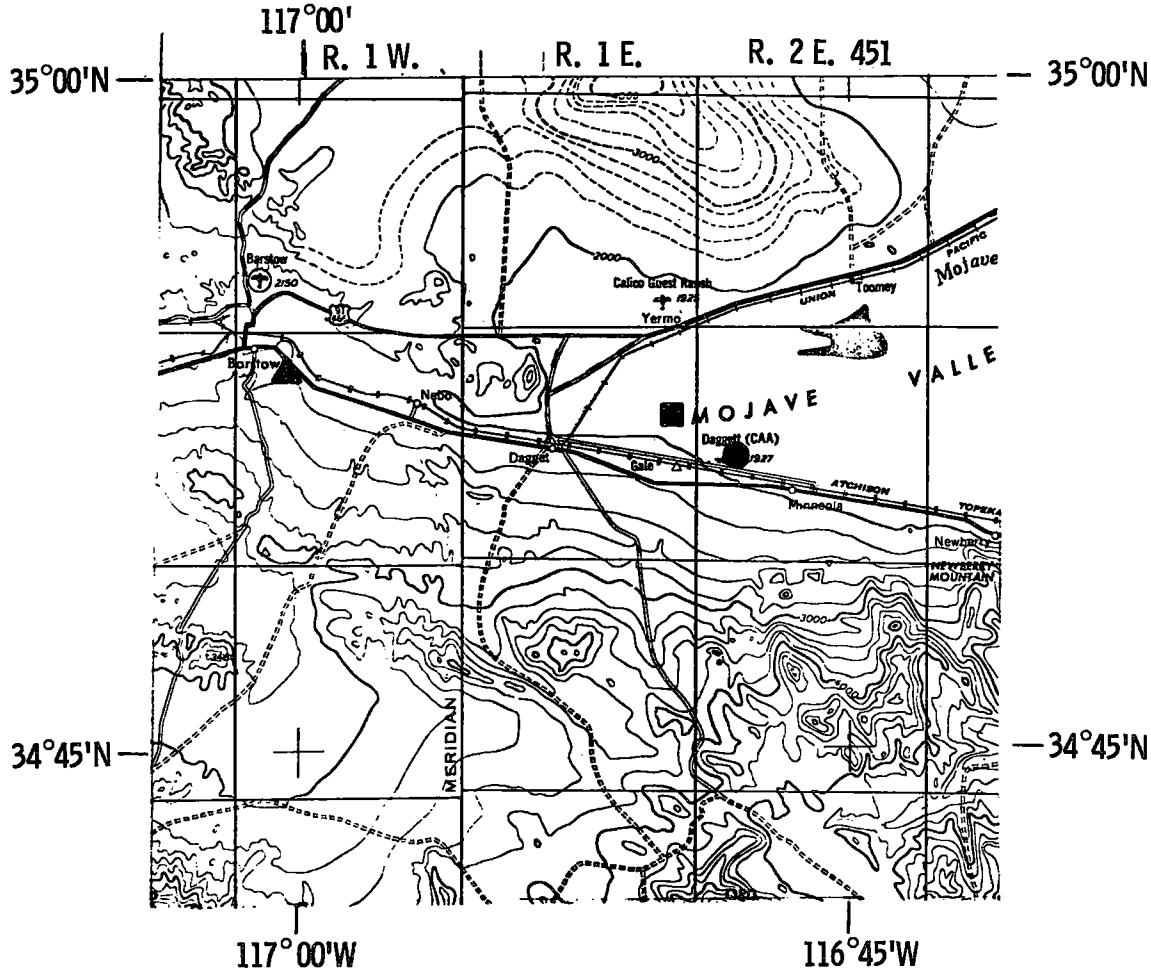

▲ SCE INSOLATION MEASURING SITE

● FAA METEOROLOGICAL OBSERVATION SITE

■ SOLAR THERMAL ELECTRIC PILOT PLANT SITE

Figure 2-3.

Dagget Insolation Variation Experiment Site

COOLWATER GENERATING STA, SO CALIFORNIA EDISON CO

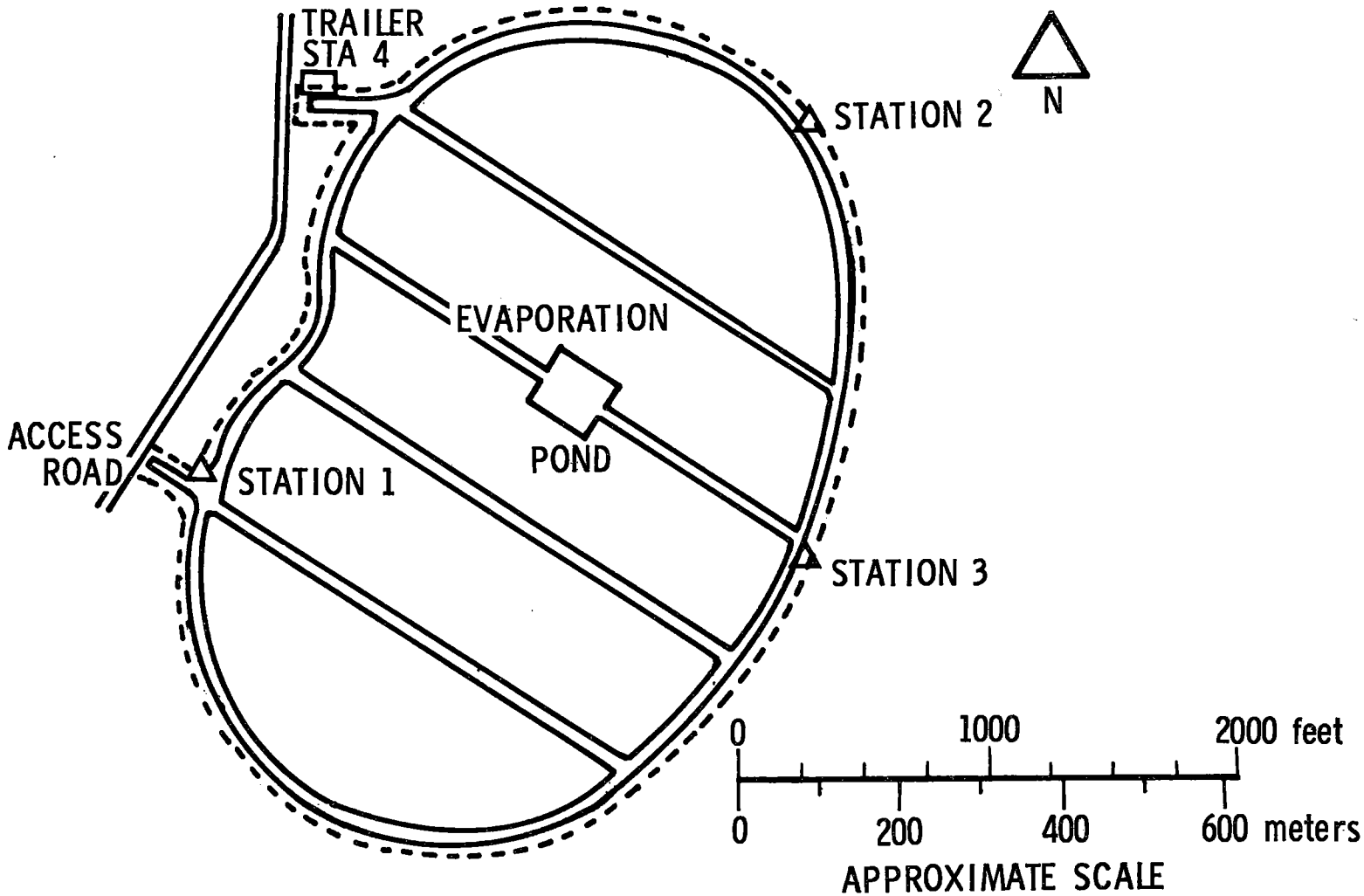

mounted with an Eppley shade ring for measuring diffuse radiation. Also located at the base station are high quality Eppley instruments: a NIP and a pyranometer (initially a model 48 and later a PSP). These devices are used for absolute energy calibration of the system.

The output signals from all the sensors are low level electrical signals requiring conditioning for reliable transmission over the distances involved in this experiment. This conditioning is accomplished with an analog-signal-to-frequency (A/F) converter (Burr Brown VFC32) located in a weather housing just below each sensor. These converters are coupled to line drivers to assure noise immune signal transmission from all stations. Details of the converters are given in Appendix A. Signals are carried from all remote sensor locations through multi-wire weatherproof cables. These same cables also provide the low voltage DC power for the signal conditioning equipment.

Inside the base station, the frequency encoded insolation signals are processed by line receivers and averaged for 16 sec intervals. A data recording system, assembled around standard Nuclear Instrumentation Modules (NIM), stores mean intensities from each sensor every 16 sec on magnetic tape with a PERTEC Model 1507-7 incremental tape recorder. A timer controls the system so that data are recorded only during daylight hours. The data tape written by this system is in a standard 7 track 556 bpi BCD coded format. Each tape record contains the date, local standard time, and 8 channels of insolation data. A block diagram of the entire system is given in Fig. 2-1.

This system has been in operation for 5 months, and no electronic component failures have occurred. However, primary 115V power failures of any duration will shut down the data acquisition system, and have occured with a frequency of ~1/mo until changes were made to the by SCE to the power line feeding the experiment.

It should be pointed out that this system was conceived, designed, and built in a period of approximately 3 months in response to an immediate need. Therefore many design decisions were based upon procurement and assembly time constraints rather than consideration of optimum hardware.

D. SYSTEM ACCURACY

The quality of the insolation data produced by the system is determined by two factors: a) the calibration or degree of certainty associated with converting output signals to absolute energy flux densities, and b) the magnitude of the noise or random signal fluctuations associated with all components not due to changes in insolation levels. The calibration procedures and noise characteristics are described in this section.

1. CALIBRATION

The experimental system contains three components with differing calibration requirements: the Eppley instruments, the Lambda instruments, and the A/F converters.

The Eppley instruments provide energy measurements based upon Eppley or NOAA calibrations. During clear or totally overcast periods, insolation levels are constant over the sensor field and the Lambda pyranometers can be calibrated to the Eppley instruments. The direct insolation instrument, an Eppley NIP, S/N 16619E6, has been calibrated at 8.71×10^{-6} volts/Wm^{-2} by NOAA. This calibration forms the basic standard for our system. Two high-quality Eppley pyranometers are presently deployed for global reference measurements, and they have been calibrated against the NIP. An Eppley Model 8-48 pyranometer, S/N 15902, has been installed from the beginning of the experiment; the factory calibration of this instrument is 10.54×10^{-6} V/Wm^{-2}. Using an occulting disc to observe the change in instrument output when the direct solar beam is

turned on and off, we verified this calibration to be correct within 2%. The second pyranometer, an Eppley Precision PSP, S/N 17440F3, has a reported calibration coefficient of 9.71×10^{-6} V/Wm^{-2}, which we have verified to ~3% near solar noon. The larger uncertainty associated with the PSP is due to fewer calibrations on our part and a cosine response phenomenon in the PSP sensor (Ref. 15).

The Lambda LI-200S pyranometers were studied in the laboratory even though they are in fact calibrated in operation during clear hours by the Eppley model 8-48, pyranometer. Calibration coefficients ranging from 79.7 to 87.3 μamp/kWm^{-2} reported by Lambda Instruments were found to be reasonable when the output signals of the Lambdas were compared to the Eppley model 8-48, near solar noon. Preliminary data analyses described in Chapter III have been performed using a 1.05 multiplying adjustment factor with the factory calibration coefficients in order to get improved agreement between the Lambda and Eppley units. This factor of 1.05 was obtained by comparison with the Eppley model 8-48, during clear weather at Barstow.

The A/F converters were carefully calibrated in the laboratory over the range -20°C to + 60°C and found to change less than 1%. Typical current to frequency converters for the Lambda pyranometers have a calibration coefficient of 95 Hz/μA. The voltage to frequency converters used with the Eppley instruments have a typical coefficient of 900 Hz/mV. Calibration of the A/F units in the field using known voltage and current sources has shown that the calibration coefficients have so far remained within 1% of the laboratory values (see Appendix A).

2. NOISE

The stability and noise immunity of the A/F converter system are critical to the reliability of data from the entire experiment. The short term stability is tested by temporarily replacing the sensor in the field with a battery driven current or voltage

source of known magnitude. Over periods of several minutes the frequency recorded every 16 seconds on the tape is constant to 2 parts in 10^4. This may well be limited by the stability of the source circuit, rather than the A/F circuity. We believe therefore that all changes in recorded signals occurring over periods of several minutes are due to real changes in output of the associated insolation sensors.

Signals from the sensors under zero-insolation conditions produce a few Hz in the A/F converter outputs. This background noise has been rechecked in the field several times and so far remains unchanged.

III. DATA ANALYSIS

A. INTRODUCTION

The several thousand insolation measurements recorded by this experiment each month must be summarized into parameters required for the design of the pilot plant. The data provided by this experiment impacts the power plant design in several areas: thermal cycling of receiver components, variations in the quantities of heat available, and control system design, involving both the master control system and the individual receiver panel controllers. The data must be analysed to provide quantitative information for plant design in these areas, and to provide an estimate of the frequency of occurrence of cloud induced conditions which would lead to a controlled turn down of the pilot plant. Estimates of the frequency of occurrence are best made when more than a few months of data are available and so this initial report is directed towards a quantitative specification of the insolation variation.

The insolation variation specification may be made in two ways: a) the description of "typical" insolation variation events by a time sequence of insolation values on a grid superimposed on the collector field, and b) statistical measures of insolation variation, such as rates of change and rms deviations over the collector field. This report concentrates on the second approach, in the belief that statistical measures will be needed in the design process earlier than sequential specifications. Furthermore it is the statistical measures which will be used to determining what constitutes a "typical" insolation variation sequence.

At the beginning of this work the most desirable statistical descriptors were unknown. To determine the optimum descriptors we have extensively analysed four time periods, rather than all of the cloudy periods which have occurred since the experiment

went into operation. The description of these periods is contained in Section E of this Chapter. Section B describes the initial data screening procedure while section C presents a method for calculating the direct insolation at stations 1, 2 and 3. The effective mean cloud velocity and the concept of a "psuedo-station" are introduced in Section D.

B. INITIAL DATA SCREENING, CLEAR AND CLOUDY PERIODS

Data tapes containing insolation measurements from Barstow arrive approximately weekly at Aerospace. In the initial processing, the recorded measurements are converted to energy units and an entire month of the converted data is stored on a single reel of tape. At the same time the data are checked for consistency and prepared for visual inspection by plotting each day's results on a high-speed printer. Typical printer displays for clear and partly cloudy periods are shown in Figs. 3-1 and 3-2.

Partially cloudy periods are identified by rapid variations in the insolation levels, totally overcast periods are identified by very low values compared to the expected clear day values, and clear periods are identified by smooth and slow changes in insolation. It is obvious from the last definition, that a hazy period in which the insolation is slightly reduced from its clear day value, but which changes only slowly, is not differentiated from a clear period. A summary of the clear and cloudy periods for August, September and October obtained by a visual inspection of the printer plots, is shown in Figs. 3-3, 3-4 and 3-5. The narrow horizontal lines cover the clear periods, thick lines cover partial or totally overcast periods and the periods not covered by any line are times when no information was recorded.

During the month of August a total of 32 hours of cloud activity was recorded. This is about 8% of the total daylight hours for the month. During September and October, 31 and 33 hours of cloud activity were recorded. In each case this was about

FIGURE 3-1. **Raw Data Display**

OCTOBER 1978 CLEAR

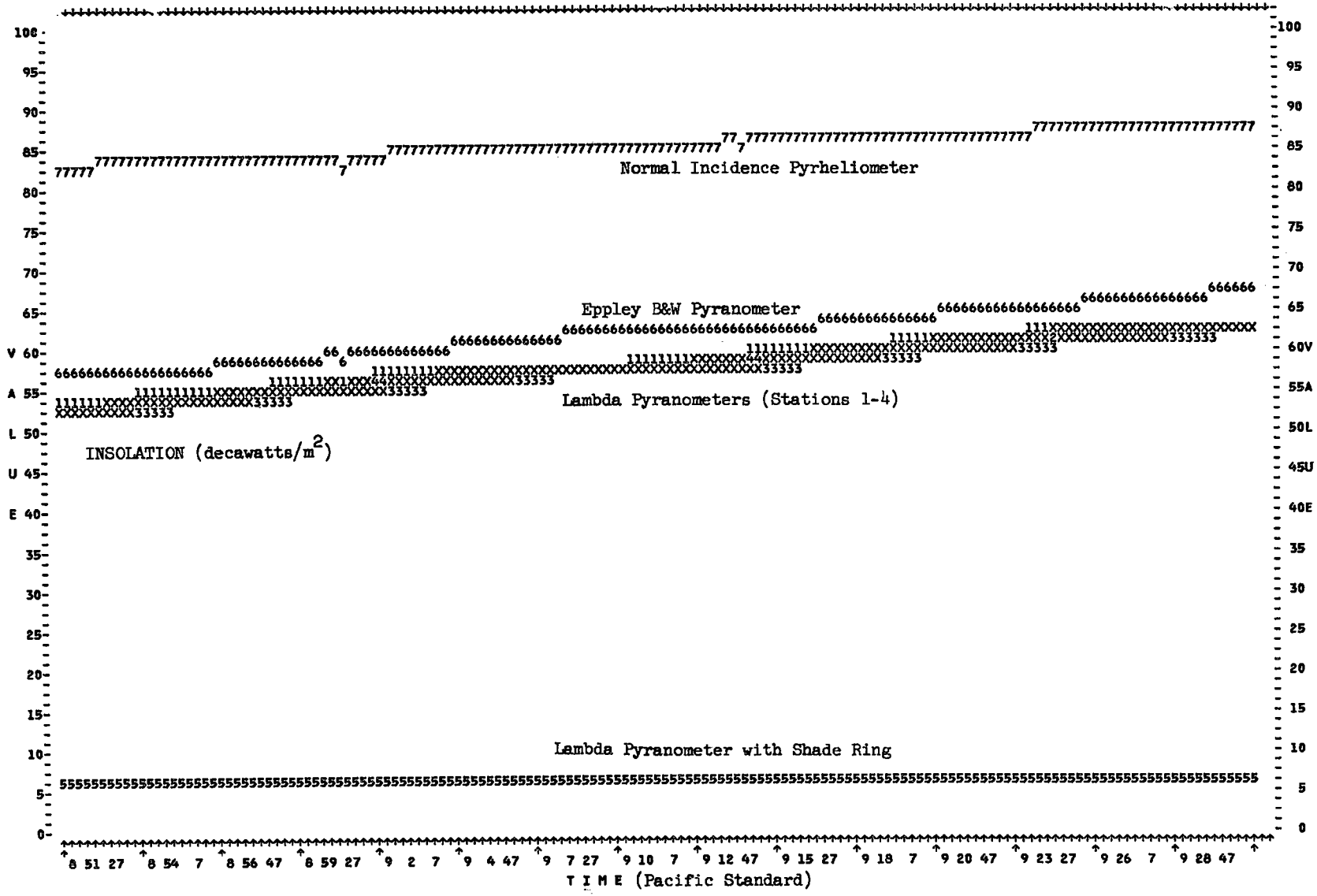

FIGURE 3-2. **Raw Data Display**

8 OCTOBER 1978

0.2-0.3 OPAQUE SKY COVER

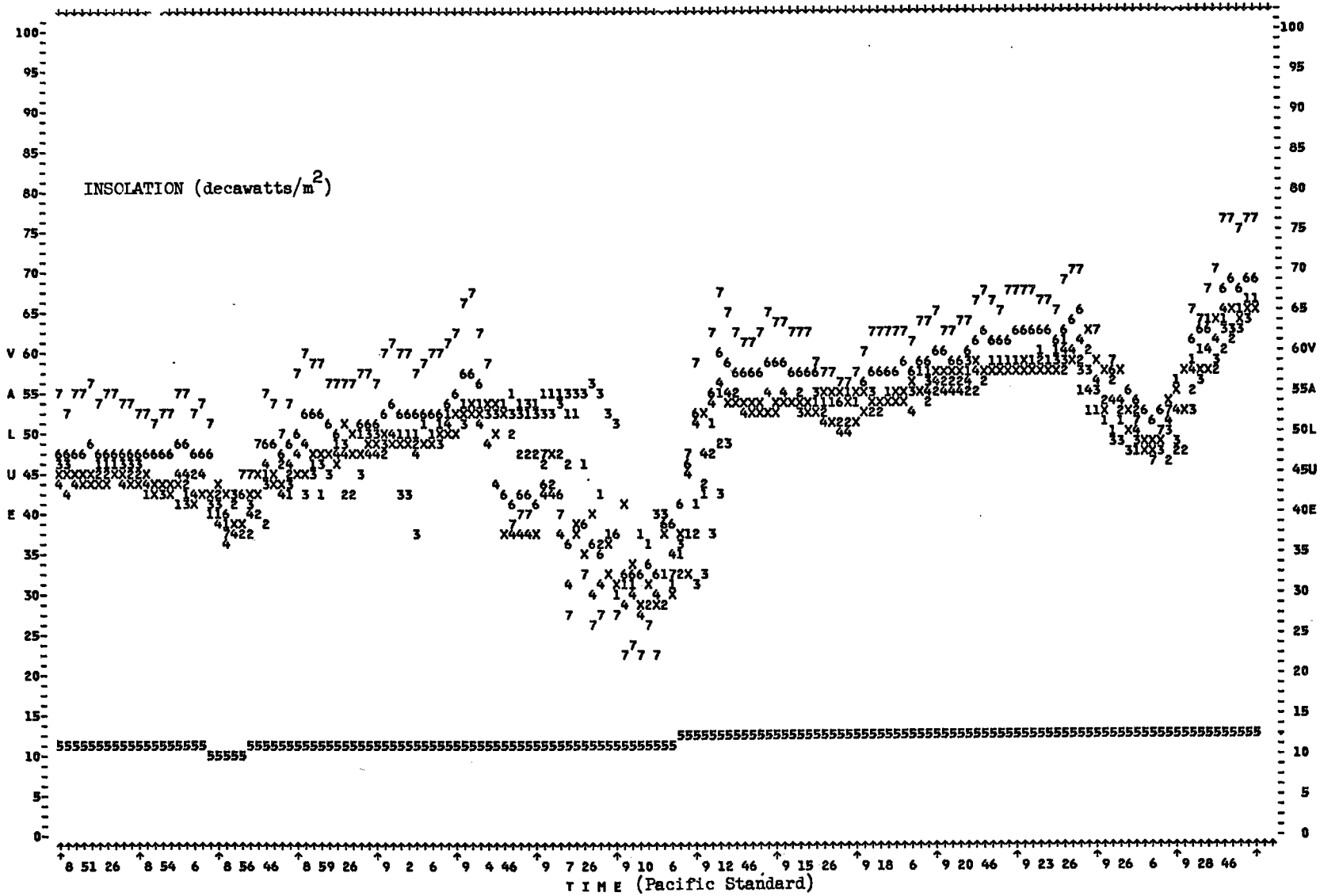

Figure 3-3.

Insolation Variation Experiment

DATA SUMMARY AUGUST

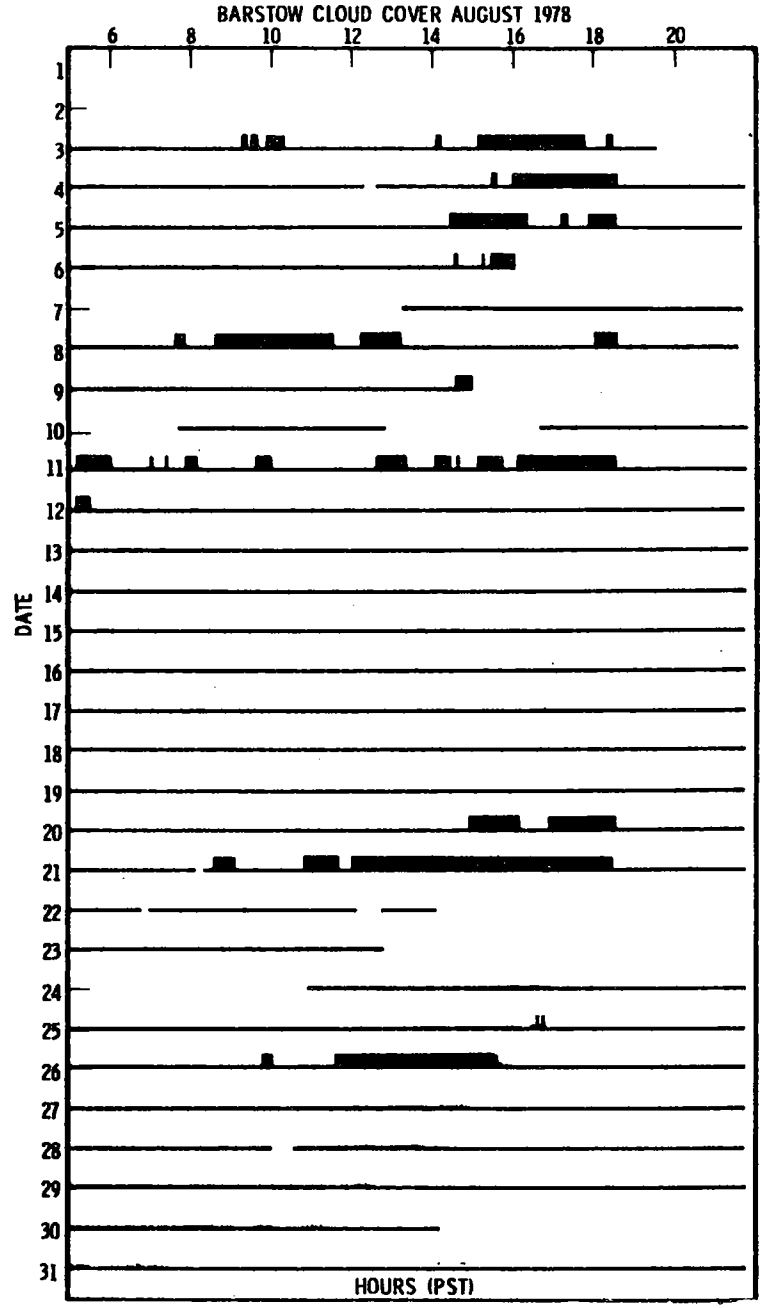

Figure 3-4.

Insolation Variation Experiment

DATA SUMMARY SEPTEMBER

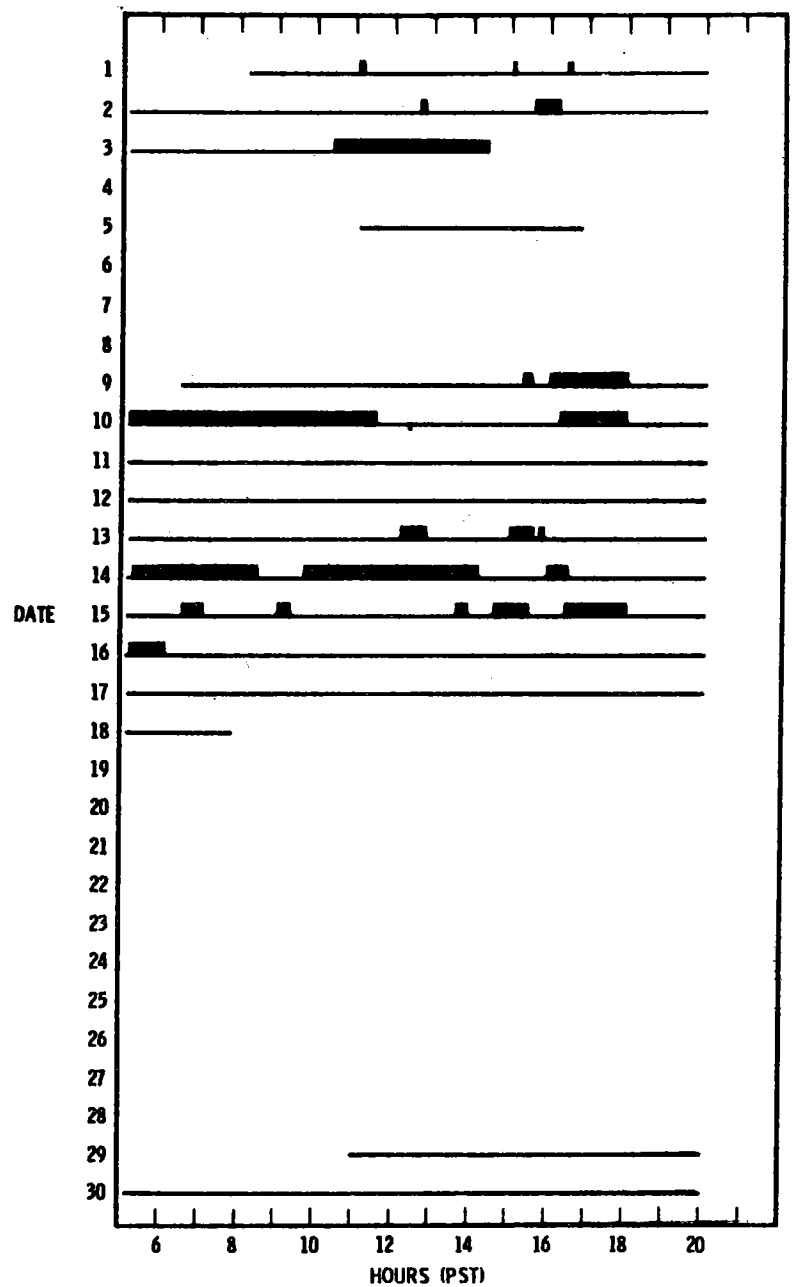

Figure 3-5.

Insolation Variation Experiment

DATA SUMMARY
OCTOBER 1978

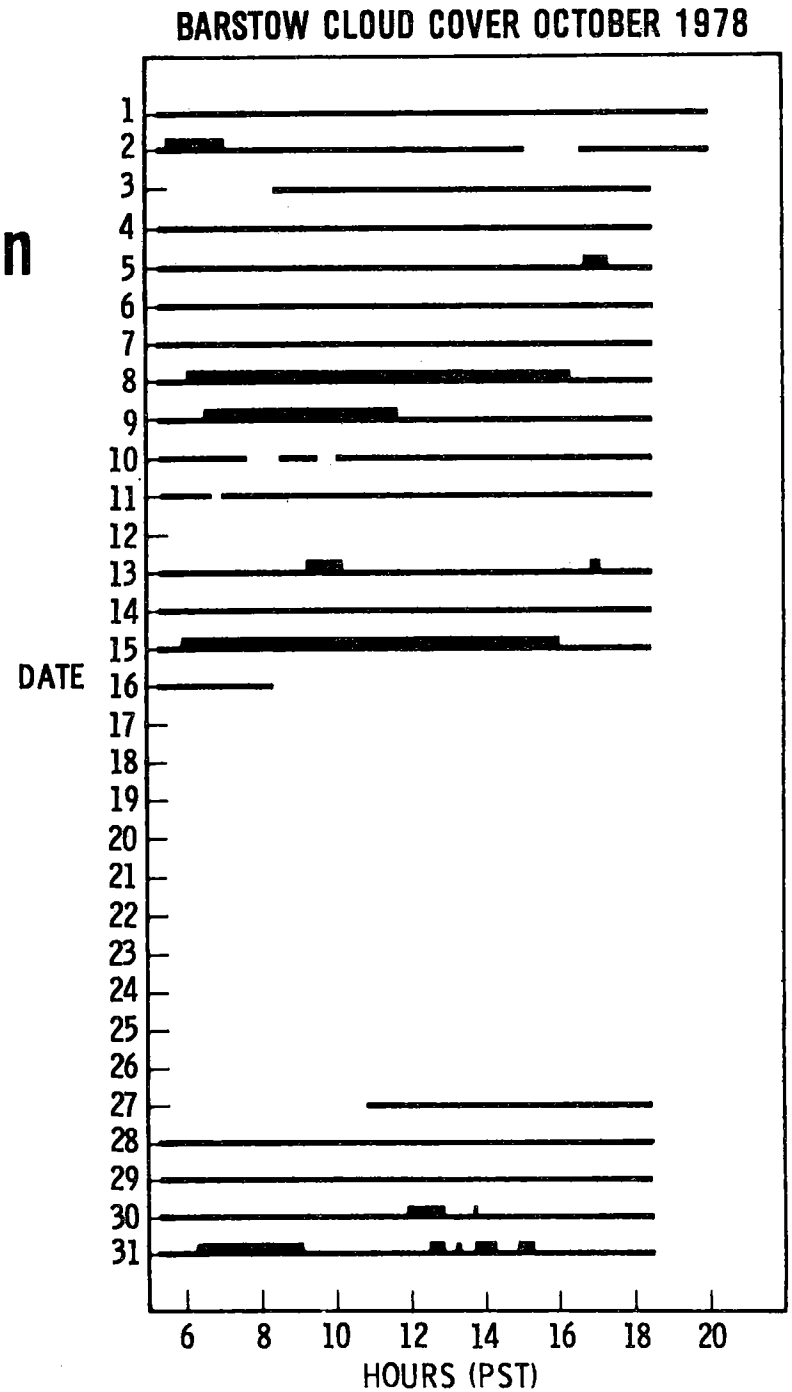

15% of the total recorded daylight hours. These figures are compared to the 1948-1976 sky cover data in Table 3-1. (The sky cover data in this table is just (100-p) where p is the percent clear sky given in Table 1-1.) The insolation-determined percentages are less because they include only those periods in which clouds cast shadows over the instruments whereas the sky cover data count any time a cloud was present anywhere in the sky.

C. DIRECT INSOLATION DETERMINATION

Direct insolation is measured by a normal incidence pyrheliometer at station 4 only and is calculated from global measurements at the other three stations. Global insolation is measured at each of the four stations with a relatively inexpensive Lambda pyranometer. In addition, measurements from the calibrated Eppley pyranometer at station 4 are recorded for the purpose of calibrating the Lambda instruments. This calibration can be made during any cloud free period when the global insolation is the same at all stations. The diffuse insolation is measured at station 4 by a Lambda pyranometer with a shade ring and is assumed to have the same value at all the stations. The relation between direct, global and diffuse insolation is

$$Q_i = D_i \cos(z) + d, \qquad i = 1, 2, 3, 4, \tag{1}$$

where z is the zenith angle of the sun, which can be computed from the time (Ref. 16), d is the diffuse insolation, Q_i is the global insolation, D_i is the direct insolation and the subscript i is the station number. During the first two months of operation we did not

Table 3-1

DAGGETT CLOUDINESS

PERCENT OF DAYLIGHT OBSERVATIONS

MONTH	SKY COVER 1948- 76 DATA	1978 INSOLATION OBSERVATIONS
AUGUST	40	8
SEPTEMBER	29	15
OCTOBER	39	15

have the shade ring instrument to measure the diffuse insolation; therefore, this quantity was calculated indirectly from the direct and global insolation available at station 4, using the relationship

$$d = Q_4 - D_4 \cos(z). \tag{2}$$

This is then substituted back into Eq. (1) and the resulting equation is solved for D_i at stations 1, 2 and 3. The result is:

$$D_i = D_4 + \frac{Q_i - Q_4}{\cos(z)}. \tag{3}$$

In actual practice the formula we use is

$$D_i = D_4 + \frac{1.05\,(Q_i - Q_4)}{\cos(z)}, \tag{4}$$

where Q_i and Q_4 are the global insolation values measured by the Lambda pyranometers. The factor 1.05 was determined by several calibration tests on clear days (See Chapter II). We believe the direct insolation at stations 1, 2, and 3 calculated by this formula are accurate to about $\pm$ 0.1 Kw/m^2 when the zenith angle is not near sunrise or sunset.

D. EFFECTIVE WIND VELOCITY DESCRIPTION

Fig. 3-6 shows the direct insolation at each of the four stations during a partially cloudy period on 8 August. A comparison of these traces reveals gross similarities and detailed differences. We postulate that the similarities are due to the passage of the

Figure 3-6.

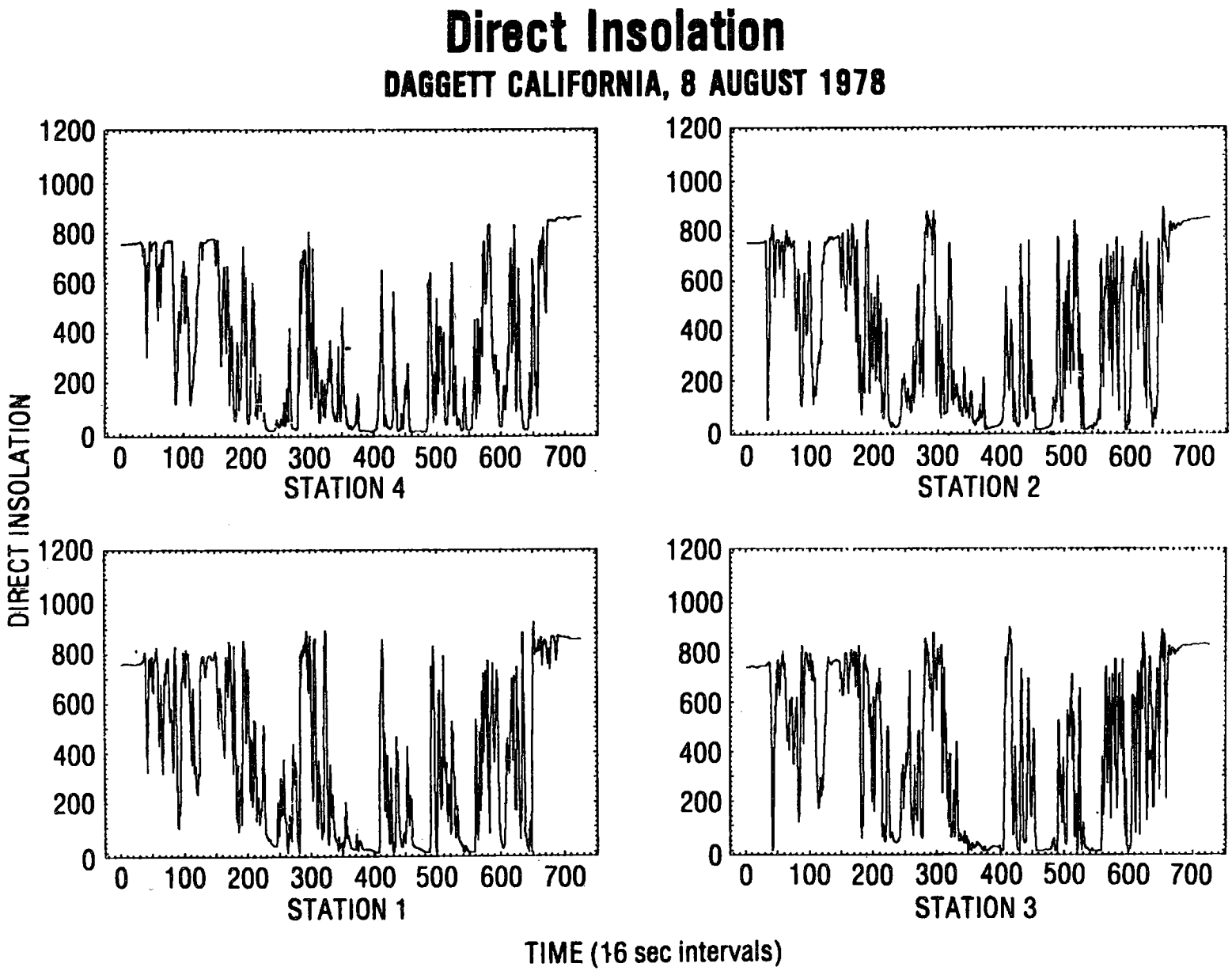
Direct Insolation
DAGGETT CALIFORNIA, 8 AUGUST 1978
DIRECT INSOLATION
1200
1000
800
600
400
200
0
0 100 200 300 400 500 600 700
STATION 4
STATION 2
STATION 1
STATION 3
TIME (16 sec intervals)

same or nearby cloud shadows over the sensors. In our analysis we assume that the overall cloud pattern does not change during its passage over the field, that is, that the pattern as a whole is moving with some velocity with respect to the ground. If this assumption is true, then the insolation measured at a station will be repeated at a delayed time at a station located directly downwind from the first station. By comparing the insolation values of these two stations one could easily determine the time delay Δt and, knowing the distance between the stations, calculate the cloud/wind velocity. In actual situations the wind velocity would rarely be parallel to a line joining two of the stations. However, if the individual clouds are large enough, we would still expect a maximum correlation between the insolation measured at one station and time shifted values of insolation at another. A quantitative measure of the correlation as a function of time shift is given by (Ref. 17)

$$C_{ij}(\Delta t) = \frac{\sum_n (Q_i(t_n) - \langle Q_i \rangle)(Q_j(t_{n+m}) - \langle Q_j \rangle)}{\left\{ \sum_k (Q_i(t_k) - \langle Q_i \rangle)^2 \sum_n (Q_j(t_{n+m}) - \langle Q_j \rangle)^2 \right\}^{1/2}}, \quad (5)$$

where $Q_i(t_n)$ and $Q_j(t_{n+m})$ are the insolation values at stations i and j, $\langle Q_i \rangle$ and $\langle Q_j \rangle$ are mean values of these quantities and the time shift is $\Delta t = t_{n+m} - t_n$. In these calculations we have used global insolation rather than direct insolation. Fig. 3-7 shows these quantities for the pair of stations 1 and 2. The maximum of the correlation coefficient in this case is 0.84 and it occurs at a time offset of -6 time units ($\Delta t = -6 \times 16 = -96$ seconds). This calculation was carried out for all six station pairs and the results are given in Table 3-2. These data are then used to calculate the wind velocity by the following analysis.

FIGURE 3-7

Effective Wind Determination

8 AUGUST 1978 DATA

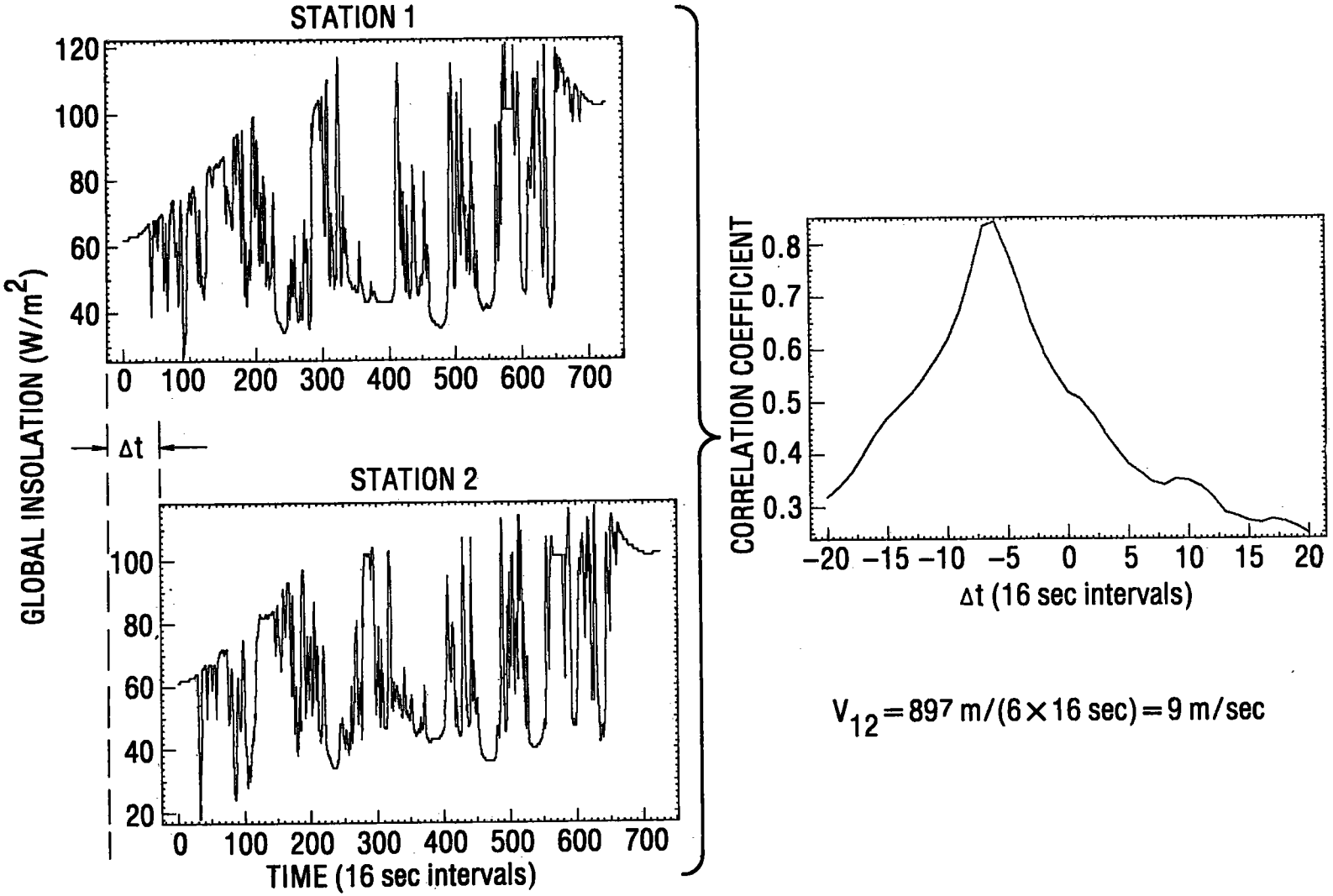

$V_{12} = 897\ m/(6 \times 16\ sec) = 9\ m/sec$

Table 3-2

EFFECTIVE WIND PEAK CORRELATION COEFFICIENTS
DAGGETT, 8 AUGUST 1978

STATION PAIR	PEAK CORRELATION	TIME OFFSET AT PEAK (sec)
2-1	0.84	96
3-1	0.74	32
4-1	0.75	48
2-3	0.68	64
2-4	0.72	48
4-3	0.61	32

Assume a value for the wind velocity vector $\vec{V}$. Also assume a semi-infinite cloud model in which the leading edge of the cloud is perpendicular to $\vec{V}$. With this simple model we can easily compute the times t_i (i = 1, 2, 3, 4) when the edge of the cloud passes over each of the stations. The time of passage $\Delta t_n = t_i - t_j$ (n = 1, 6) between the six pairs of stations is compared to the measured time shifts which are given in Table 3-2. The velocity vector is varied until the calculated and measured time shifts are in as close agreement as possible. The value of $\vec{V}$ giving the best agreement is the calculated wind velocity. We have chosen the following function as a measure of the "closeness" between the measured and calculated time shifts:

$$S(\vec{V}) = \sum_{n=1}^{6} \left| C_n^{\max} [\Delta t_n(\vec{V}) - \Delta t_n \text{ (measured)}] \right|^2. \qquad (6)$$

Here, $C_n^{\max}$ are the peak correlations and Δt_n (measured) are the time offsets given in Table 3-2. The reason for multiplying the differences between the measured and calculated time shifts by the correlation factors is to give increased weight to the more highly correlated values. The wind velocity is the value that minimizes the function $S(\vec{V})$. The effective wind velocity calculated by this formula from the data in Table 3-2 is 9 m/sec at a direction of 30° from north.

The wind velocity is useful for calculating insolation values at locations other than the four sensor stations. These additional locations are shown in Fig. 3-8. They lie on lines which pass through the stations and are parallel to the velocity vector. The insolation levels at these "psuedo-stations" are the values measured at the real stations at the earlier or later times indicated in the diagram. These additional psuedo-stations provide a better sampling of the spatial distribution of the insolation over the collector field than if we used only the four real stations.

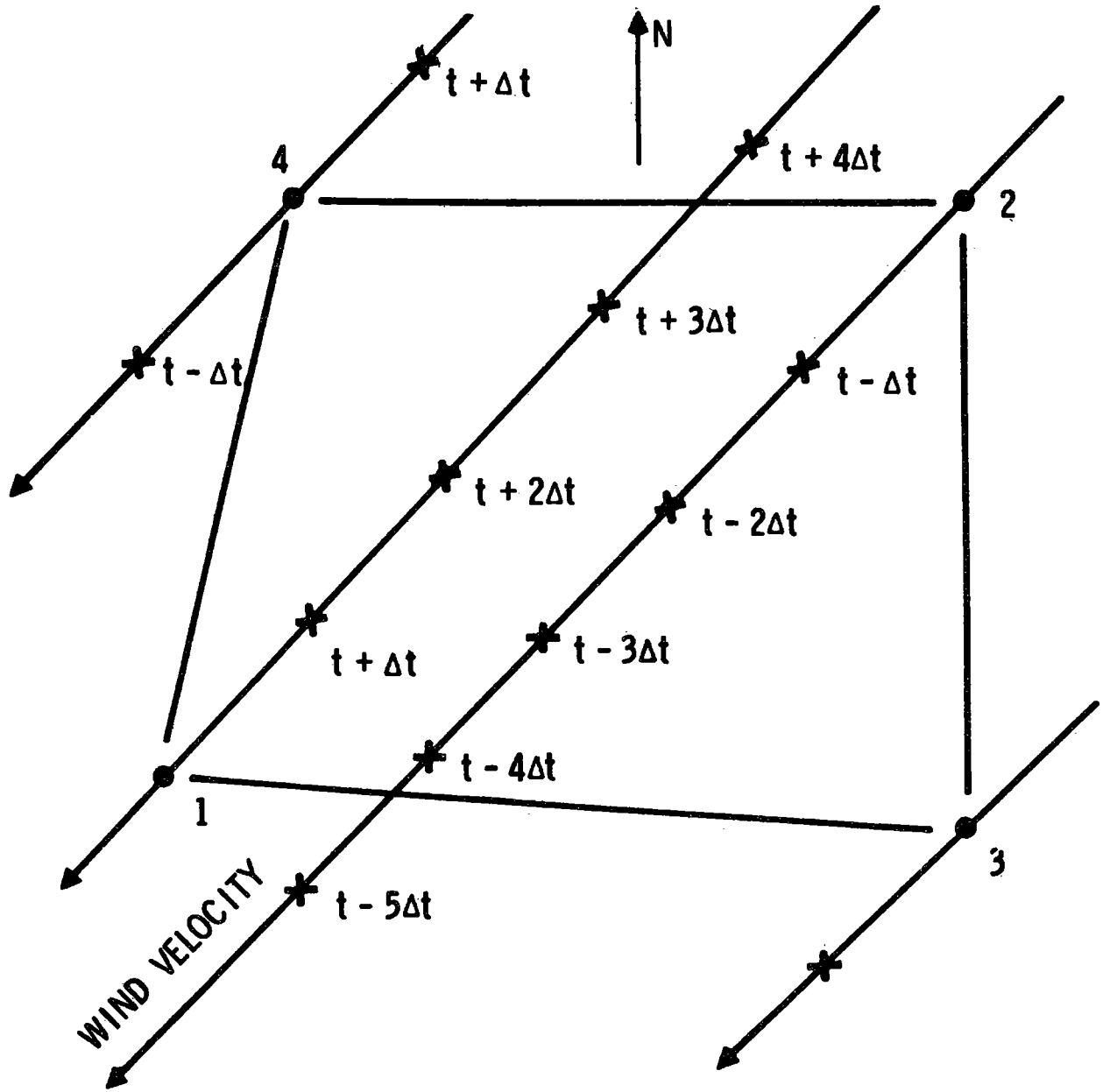

Figure 3-8. Example of Generation of "Pseudo-Stations" for use in Computing Array Averages. The example data are taken from 8 August.

A sketch of the cloud pattern passing over the collector field at about 12:30 P.S.T. on August 8 is shown in Fig. 3-9. The sizes of the clouds in the direction parallel to the velocity vector are fairly well defined but not the sizes perpendicular to the velocity. Additional data, such as cloud photographs, would allow better definition of cloud shadow profiles.

E. ANALYSIS OF SPATIAL AND TEMPORAL INSOLATION VARIATIONS

In this section a quantitative analysis will be made of the temporal and spatial variations of insolation that occurred during four partially cloudy periods in August 1978. The four periods were chosen to span a range of different types of cloud conditions. Each period was about three hours in duration and each occurred on a separate day. The direct insolation at station 4 for each of these days, August, 5, 8, 11 and 26, is displayed in Figs. 3-10 and 3-11. The data shown in Fig. 3-10 have been averaged and sampled over 15-minute intervals. This is the same resolution as the West Associates/SCE data referred to in the introduction and Fig. 1-1. In Fig. 3-11 the same data have been averaged and sampled over one-minute intervals. (The data could not be plotted at the basic 16-sec interval for an entire day because of plotter resolution limitations.) Obviously a great deal of temporal information is lost in the 15-minute averaging. A recent simulation study of the 10 MW_e plant operation (Ref. 1) indicates that the plant response time is fast enough to require data which are sampled more than once a minute.

The station 4 direct insolation, plotted at the full 16-second resolution for the four cloudy periods chosen for analysis is shown in Fig. 3-12. Time is measured in 16-sec units in these plots. The initial and final clock times (Pacific Standard Time) of each period

Figure 3-9.

Cloud Shadows Passing Experiment

8 AUGUST 1978, SPEED 9 m/sec

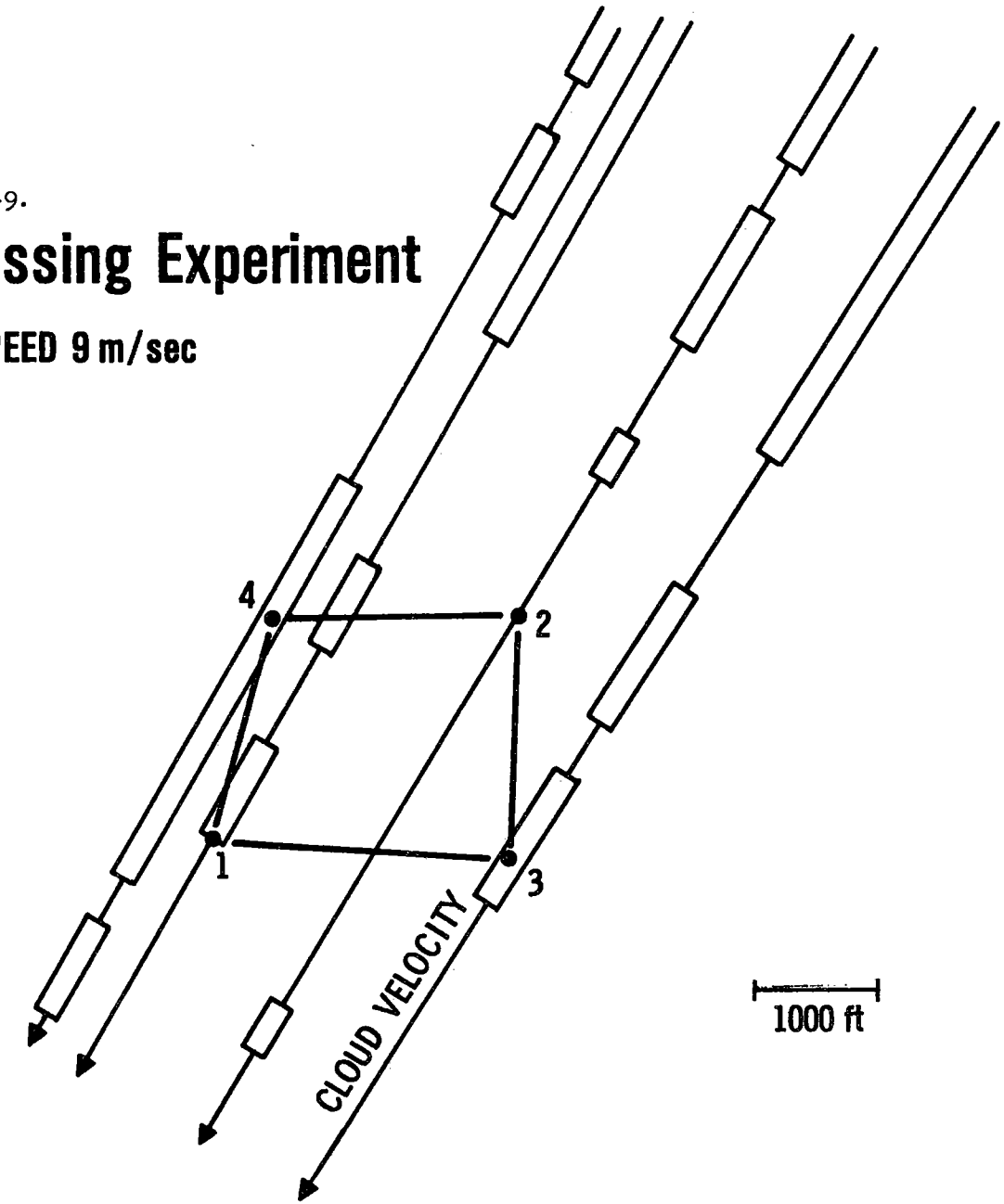

Figure 3-10.

Direct Insolation

DAGGETT CALIFORNIA, 15 MINUTE MEANS

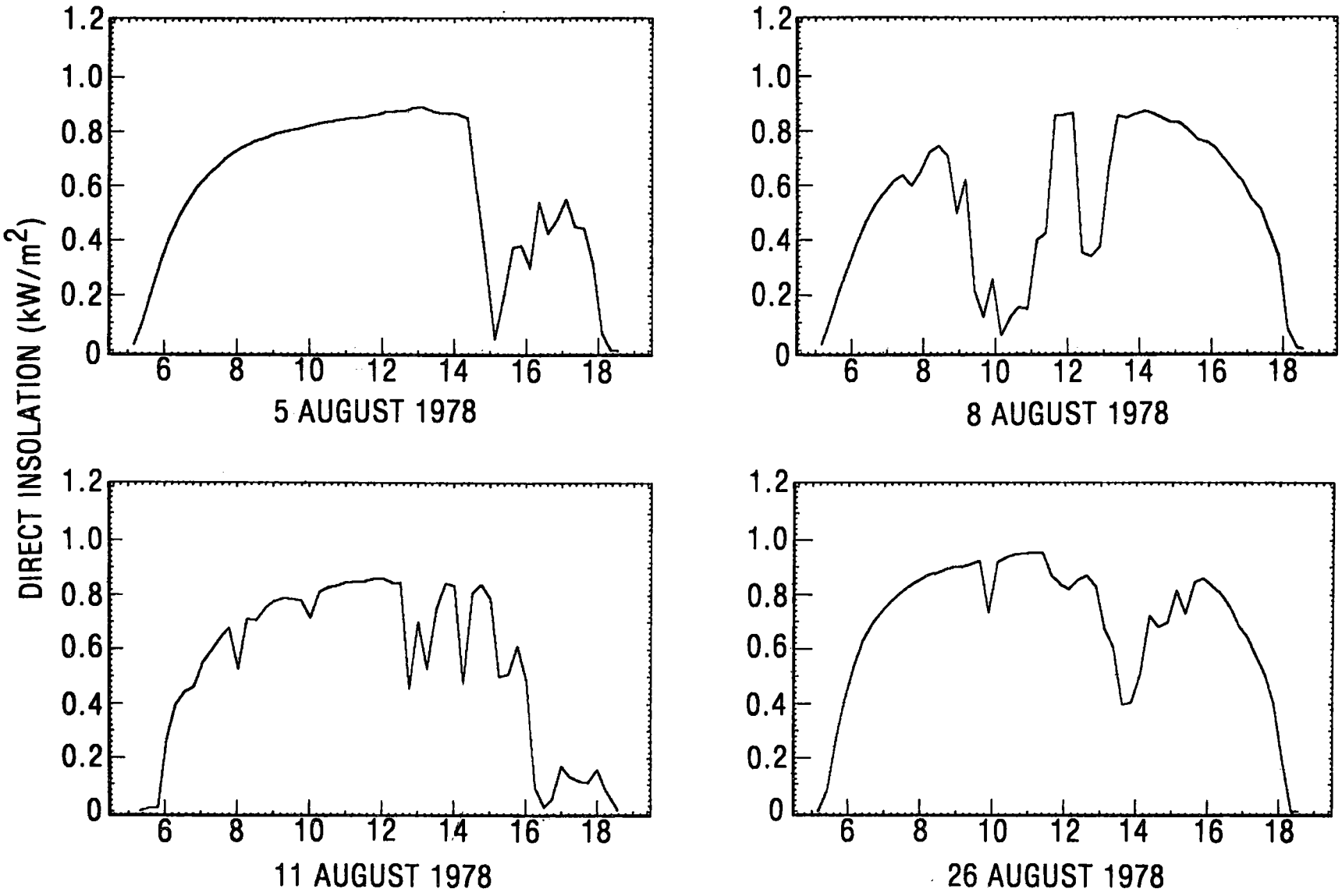

Figure 3-11.

Direct Insolation

DAGGETT CALIFORNIA, 1 MINUTE MEANS

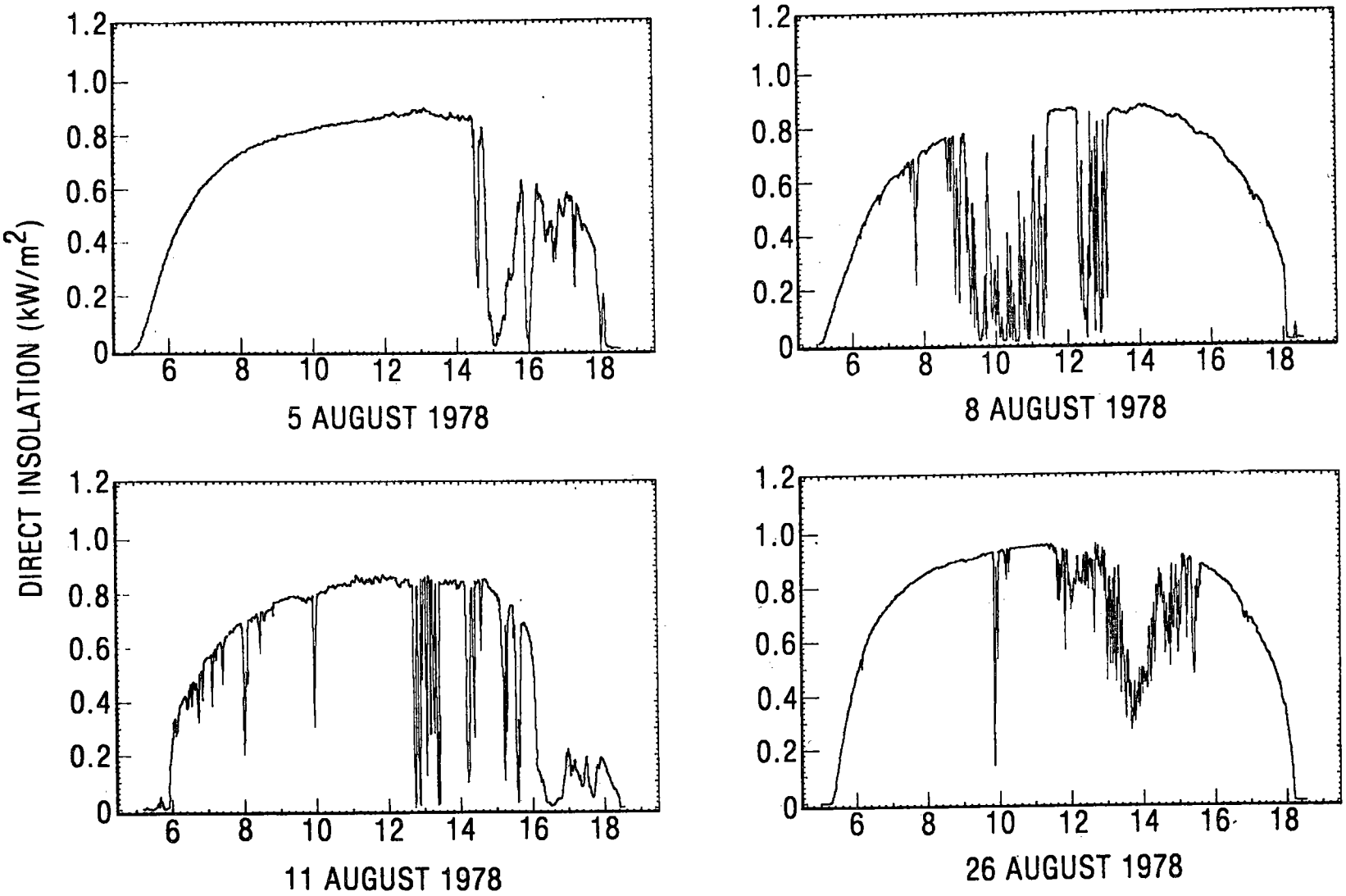

Figure 3-12.

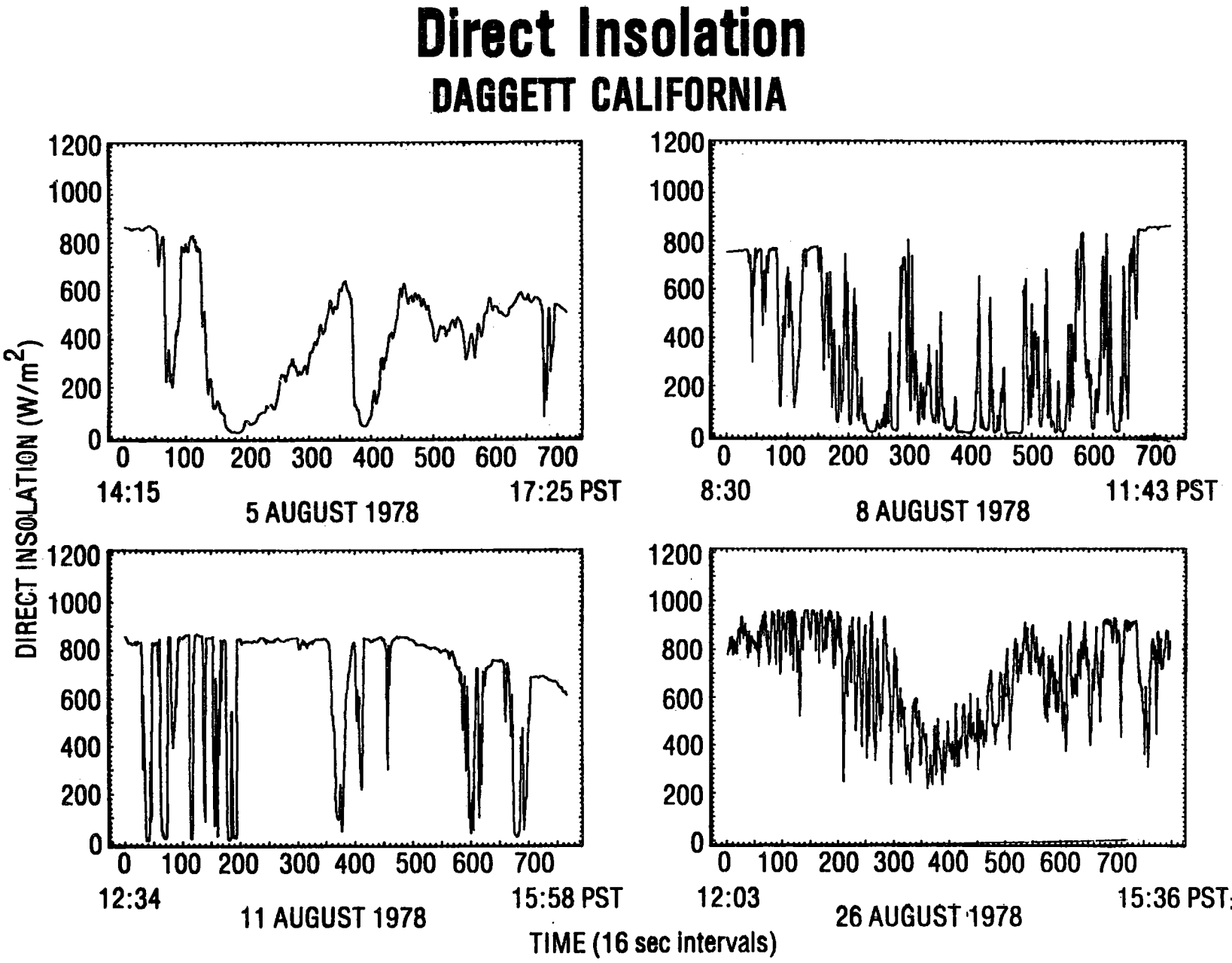
Direct Insolation
DAGGETT CALIFORNIA
DIRECT INSOLATION (W/m2)
1200
1000
800
600
400
200
0
0 100 200 300 400 500 600 700
14:15
17:25 PST
5 AUGUST 1978
8:30
11:43 PST
8 AUGUST 1978
12:34
15:58 PST
11 AUGUST 1978
12:03
15:36 PST
26 AUGUST 1978
TIME (16 sec intervals)

are also indicated in the figure to allow location of each of these cloudy intervals within the entire day traces in Fig. 3-11. The reported meteorological conditions and the calculated effective wind velocities during these periods are given in Table 3-3.

In an attempt to categorize these cloud events, the Fourier power spectrum of each of the curves in Fig. 3-12 was calculated. The results are shown in Fig. 3-13. It is not clear what information, if any, is obtainable from these plots. At the present this does not seem to be a useful approach.

The central tower of the power plant receives radiation from all the heliostats while any single panel on the tower receives radiation from a portion of the heliostat array. The control systems for each panel must be able to respond to the changing radiation level received by the panel. Summing the output of several heliostats has a smoothing effect which reduces the high frequency fluctuations. The output of a single heliostat varies the most rapidly while the average output of the entire array varies the least rapidly. A partial averaging, such as that affecting a single receiver panel, will fall somewhere between these limits. Fig. 3-14 shows a plot of the insolation at a single station and also two plots of average insolation for the 8 August data. The plot which is labeled "station 1-4 mean" is the calculated average of the direct insolation at the four real stations while the plot labeled "array mean" is calculated by also including the "psuedo-stations" in the averaging. Both of these calculated averages are estimates of the average insolation over an entire array of heliostats. The utility of the additional psuedo-stations in providing a better statistical average is evident in these calculations. Below each of the insolation traces in this figure is a histogram which shows the percent of time the insolation is at various levels. For the 8 August data, a single station tends to have a bimodal distribution; i.e., it is either on or off, with only a small time spent at various intermediate levels. Averaging tends to make the distribution more uniform.

Table 3-3

Insolation Variation Experiment

Comparison of Observation Periods

DATE	5 August	8 August	11 August	26 August
Meteorological Data				
Ceiling (kft)	5	10	6-8	25
Cloud Type	Cumulus	Cumulus	Cumulus	Cirrus
Cloud Cover (tenths)				
Opaque	5	4	2-6	2-3
Total	5	5	3-7	4-7
Effective Wind (mph)	16 SW	21 NE	19 S	80 W
Maximum Spatial RMS Deviation ≈ 400 W/m^2	Yes	Yes	Yes	200 W/m^2
Bimodal Temporal Dist	Trimodal	Yes	Yes	Skewed Normal
Temporal Distribution Independent of Averaging	Yes	Yes	Yes	Yes
$\Delta D/\Delta t$, 95 Percentile, Single Sensor (Wm^{-2} sec^{-1})	2	12	6.5	8
$\Delta D/\Delta t$ Decreases with Spatial Averaging	Yes	Yes	Yes	No
$\Delta D/\Delta t$, 95 Percentile, Array Average (Wm^{-2} sec^{-1})	1	4	3.5	4
Outage Duration Increases With Spatial Averaging	Yes	Yes	Yes	Yes

Figure 3-13. **Spectral Analysis of Direct Insolation Variation**

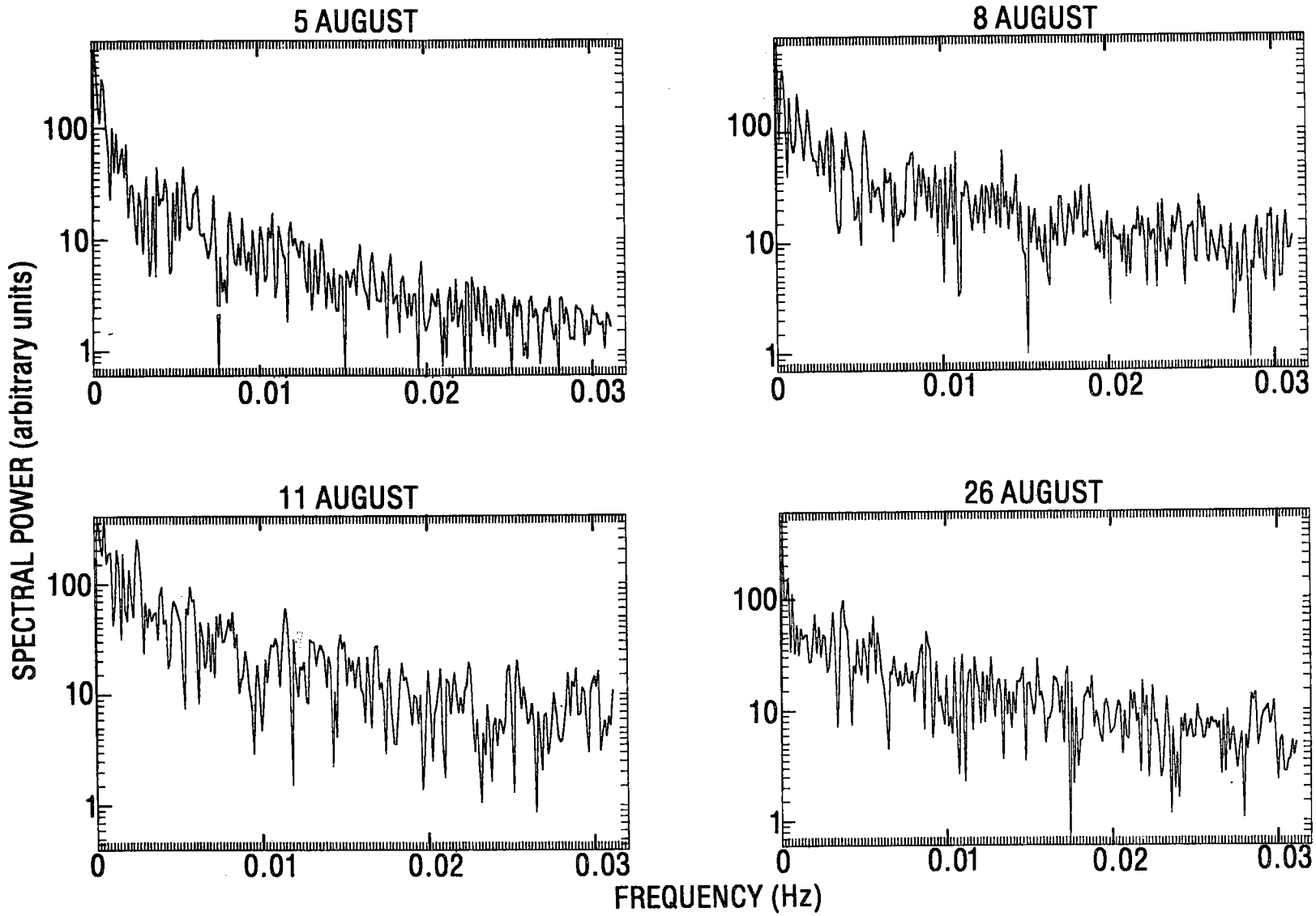

Figure 3-14.

Temporal Frequency Distribution of Direct Insolation

DAGGETT CALIFORNIA, 8 AUGUST 1978

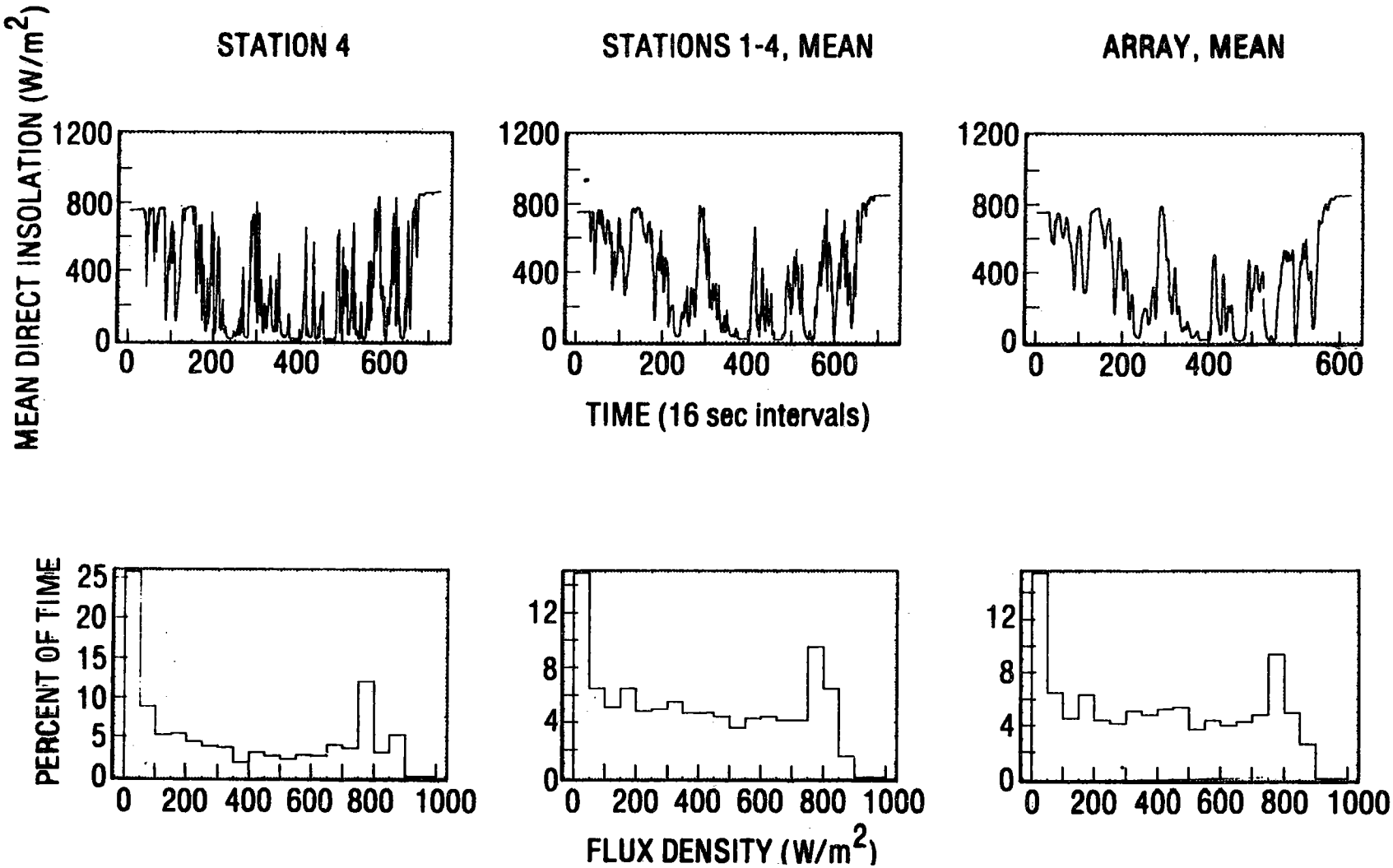

Similar plots are given in Figs. 3-15, 3-16 and 3-17 for the August 5, 11 and 26 data. The 5 August insolation did not have large high frequency fluctuations, consequently it is not effected much by the averaging. The 26 August data have very high frequency fluctuations which are greatly reduced by the averaging, although the average still varies quite rapidly. The reason for this is that the cloud shadows are moving very fast over the array. The calculated effective velocity of the high cirrus clouds is 80 miles per hour. Consequently a series of cloud shadows, each covering an area larger than the array, is moving rapidly over the array, producing a high frequency fluctuation in the total array output.

The power plant control system must respond to changes in received power, both the total power and the power received by each individual panel. Therefore it is important to establish values of the rate of change of insolation and how frequently these values occur during typical cloudy events. The rate of change (numerical first derivative) of the single station and average insolation traces displayed in Fig. 3-14 are shown in Fig. 3-18. Beneath these curves are the cumulative percentages (ogives) of the distribution of these rates. These ogives show that at the 95% level, the rate of change of insolation at station 4 (on 8 August) was 12 watts/m^{-2} sec^{-1} while for the array mean it was 4 watts m^{-2} sec^{-1}. The 95% level rates for the other cloudy periods are given in Table 3-3.

The spatial distribution of insolation over the collector field at any instant determines the distribution of power to the various panels on the central tower. A statistical parameter which measures the non-uniformity of the illumination over the array is the root mean square (rms) deviation of the insolation from its instantaneous average value, i.e.,

Figure 3-15.

Temporal Frequency Distribution of Direct Insolation

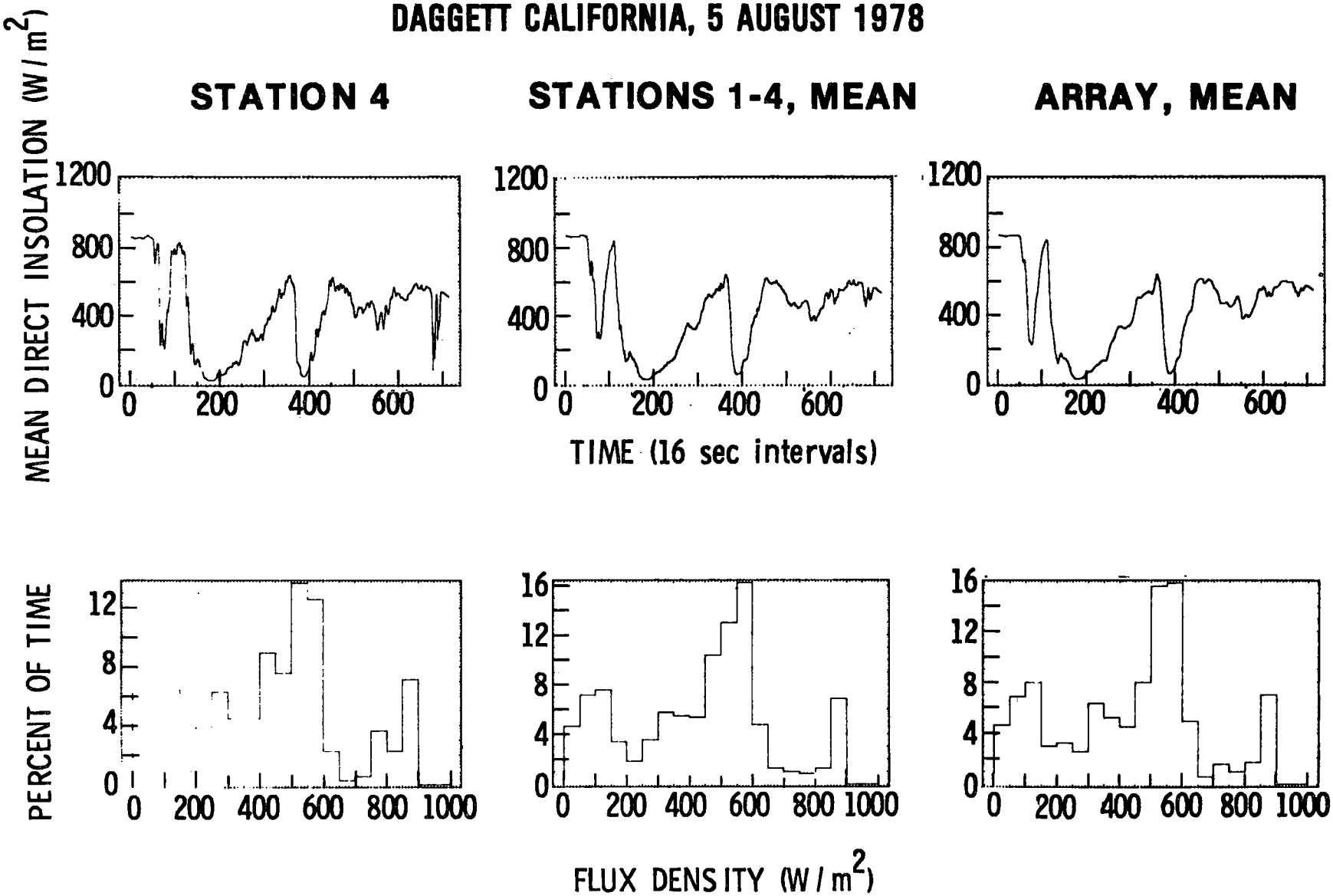

Figure 3-16.

Temporal Frequency Distribution of Direct Insolation

DAGGETT CALIFORNIA, 11 AUGUST 1978

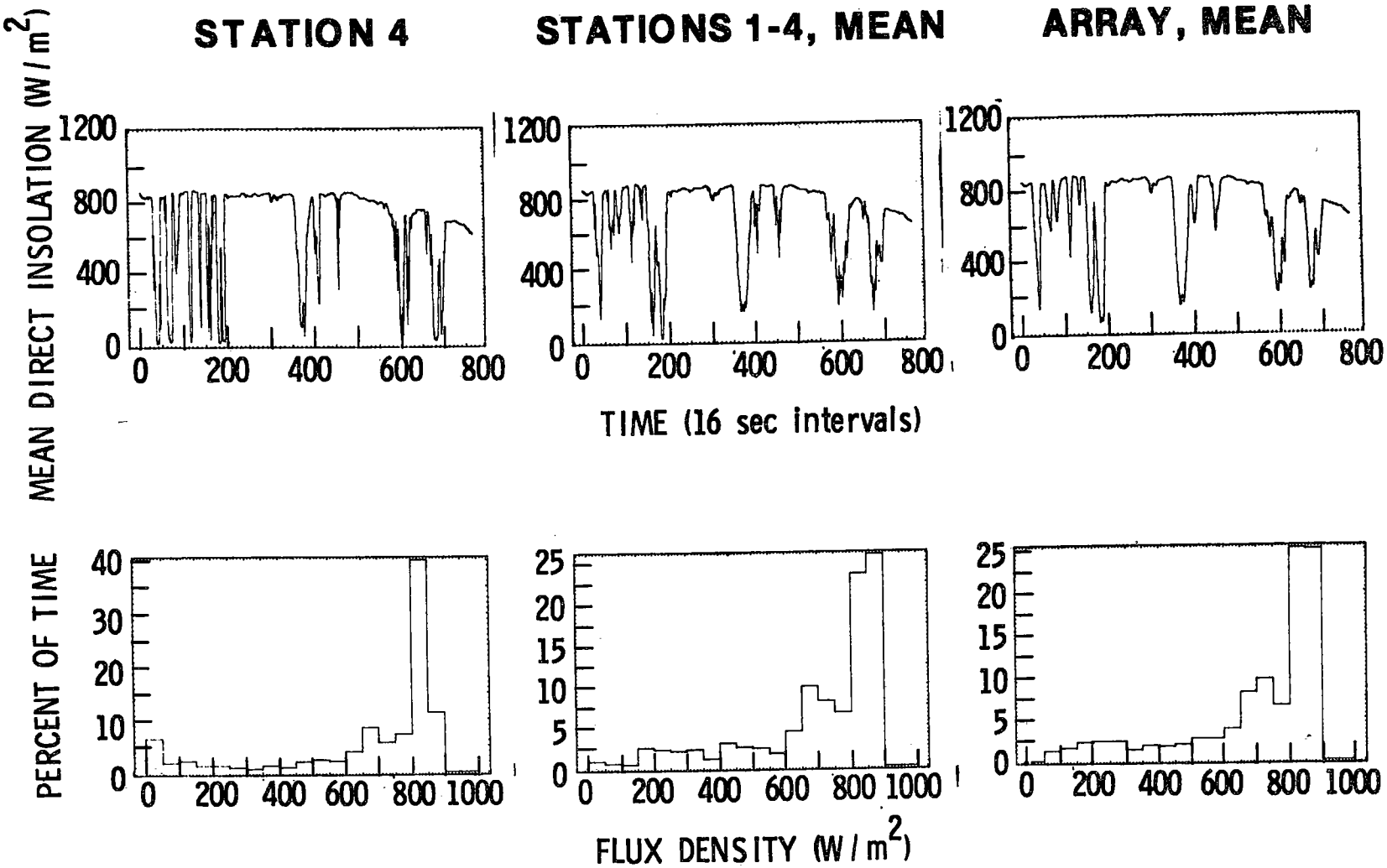

Figure 3-17.

Temporal Frequency Distribution of Direct Insolation

DAGGETT CALIFORNIA, 26 AUGUST 1978

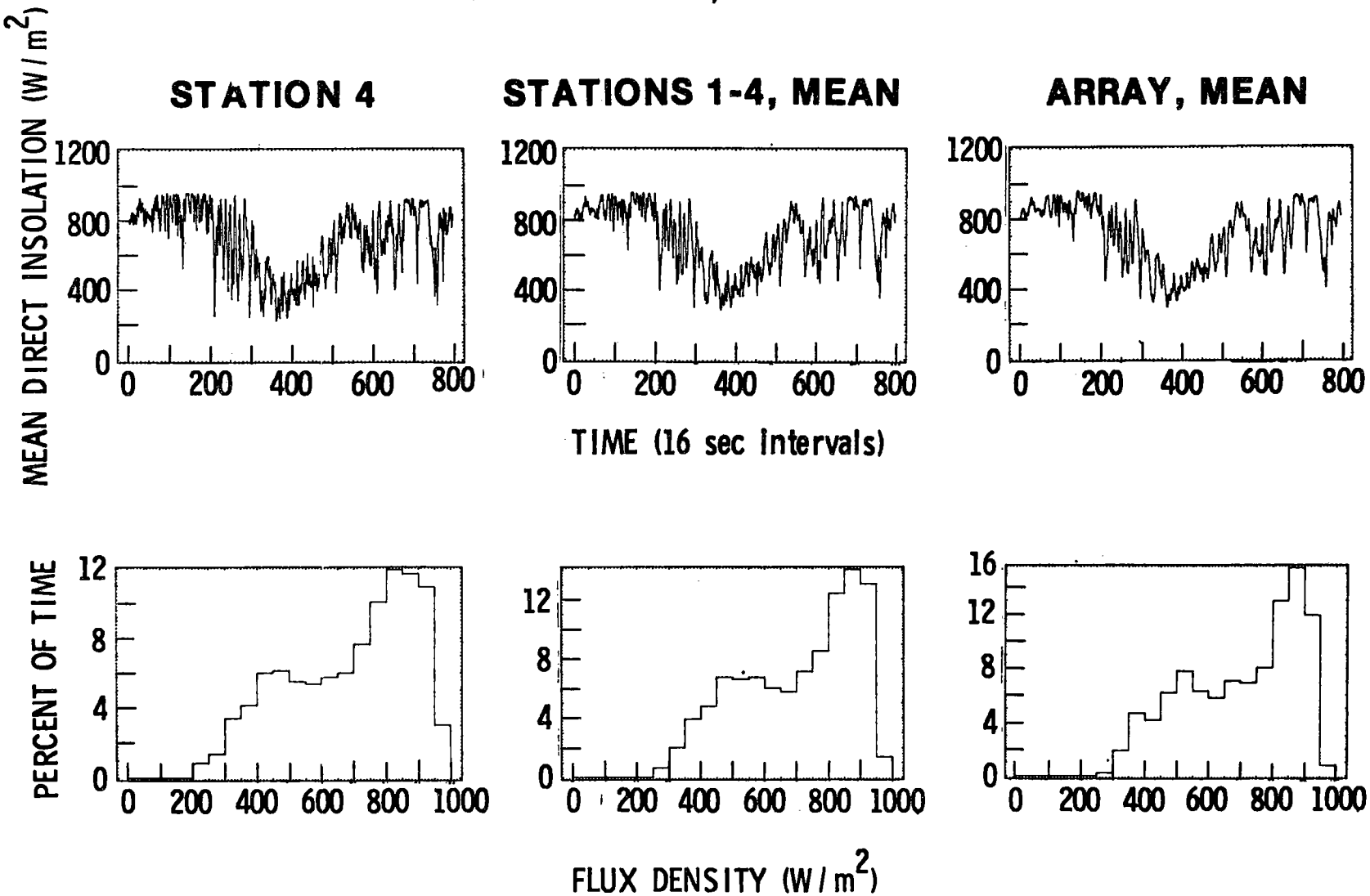

Figure 3-18.

Rate of Insolation Change

DAGGETT CALIFORNIA 8 AUGUST 1978

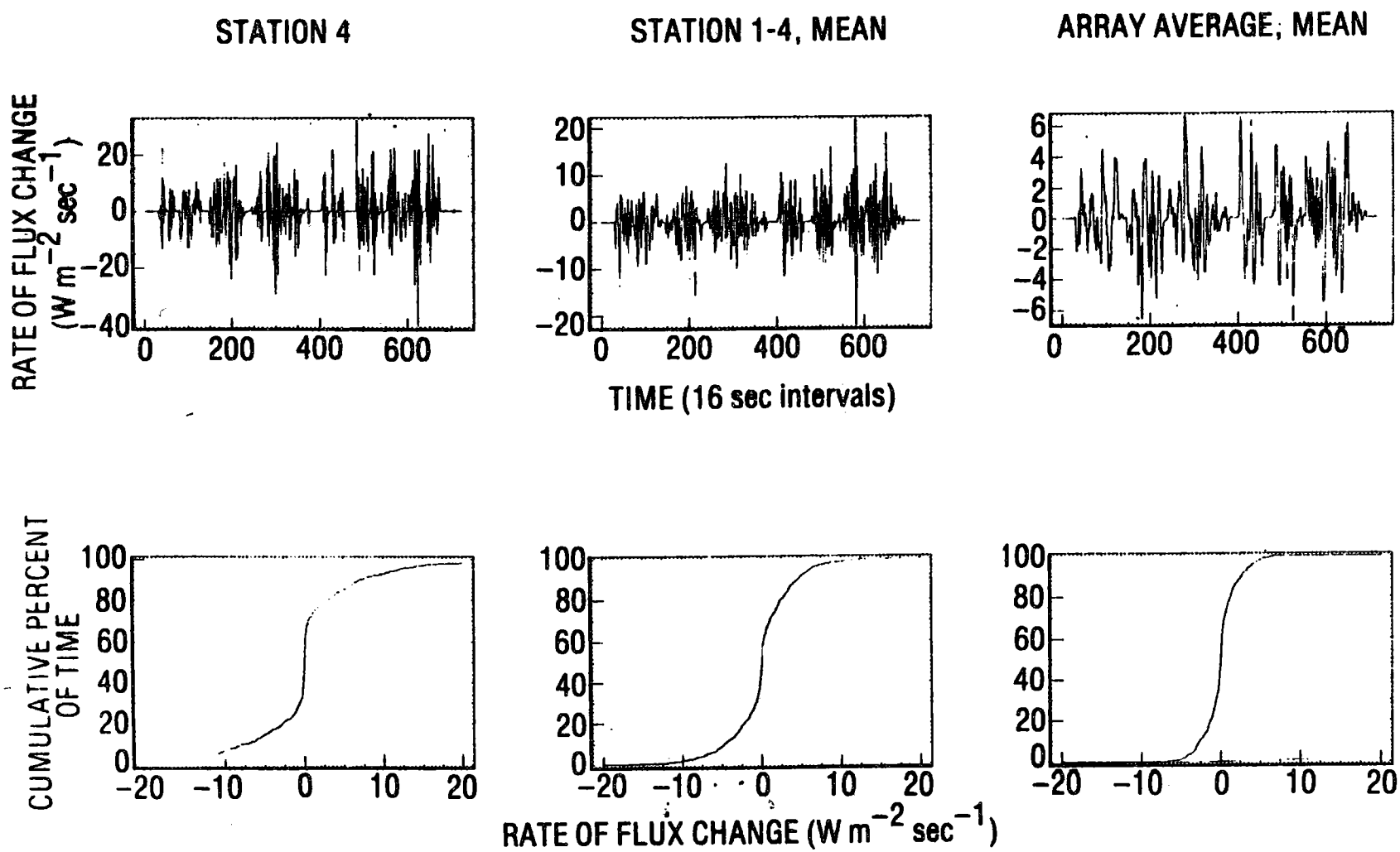

$$\sigma(t) = \left\{ \frac{1}{N-1} \sum_{i=1}^{N} \left[D_i(t) - \langle D(t) \rangle \right]^2 \right\}^{1/2}, \tag{7}$$

where N is the number of stations, D_i (t) is the insolation at station i and $\langle D(t) \rangle$ is the instantaneous average insolation over the array. Two approximations to this quantity were calculated. The first used only the insolation values at the four real stations and the second included the psuedo-station values. Both these estimates are plotted in Fig. 3-19 for 8 August data.

The parameters σ(t) alone cannot determine the distribution of insolation over the various receiver panels. Such a distribution is a complicated function of the geometry of the plant and the detailed pattern of illumination over the heliostat array. It can, however, help indirectly by placing limits on cloud models. Any cloud model which would purport to simulate the 8 August cloud period would have to produce a calculated σ(t) which is at least in qualitative agreement with the curves plotted in Fig. 3-19. Also, the calculated average of the model would have to qualtitatively agree with the array mean plotted in Fig. 3-14. The illumination calculated by such a model could then be used by a simulation program to calculate the instantaneous power distribution over the receiver panels.

A question that is of concern in both the operation and design of a solar plant is: "During a partially cloudy episode how many times does the insolation drop below a cut-off value and how long can it be expecteed to stay below this cutoff?" In order to provide some information relevant to answering these questions, the statistics of the periods of outages during which the insolation dropped below 300 W/m^2 was computed. These data are summarized in Table 3-4.

A summary and comparison of some of the quantities calculated for all four periods, along with some meteorological data, are given in Table 3-3.

Figure 3-19. **Temporal Insolation Variation**

DAGGETT CALIFORNIA, 8 AUGUST 1978

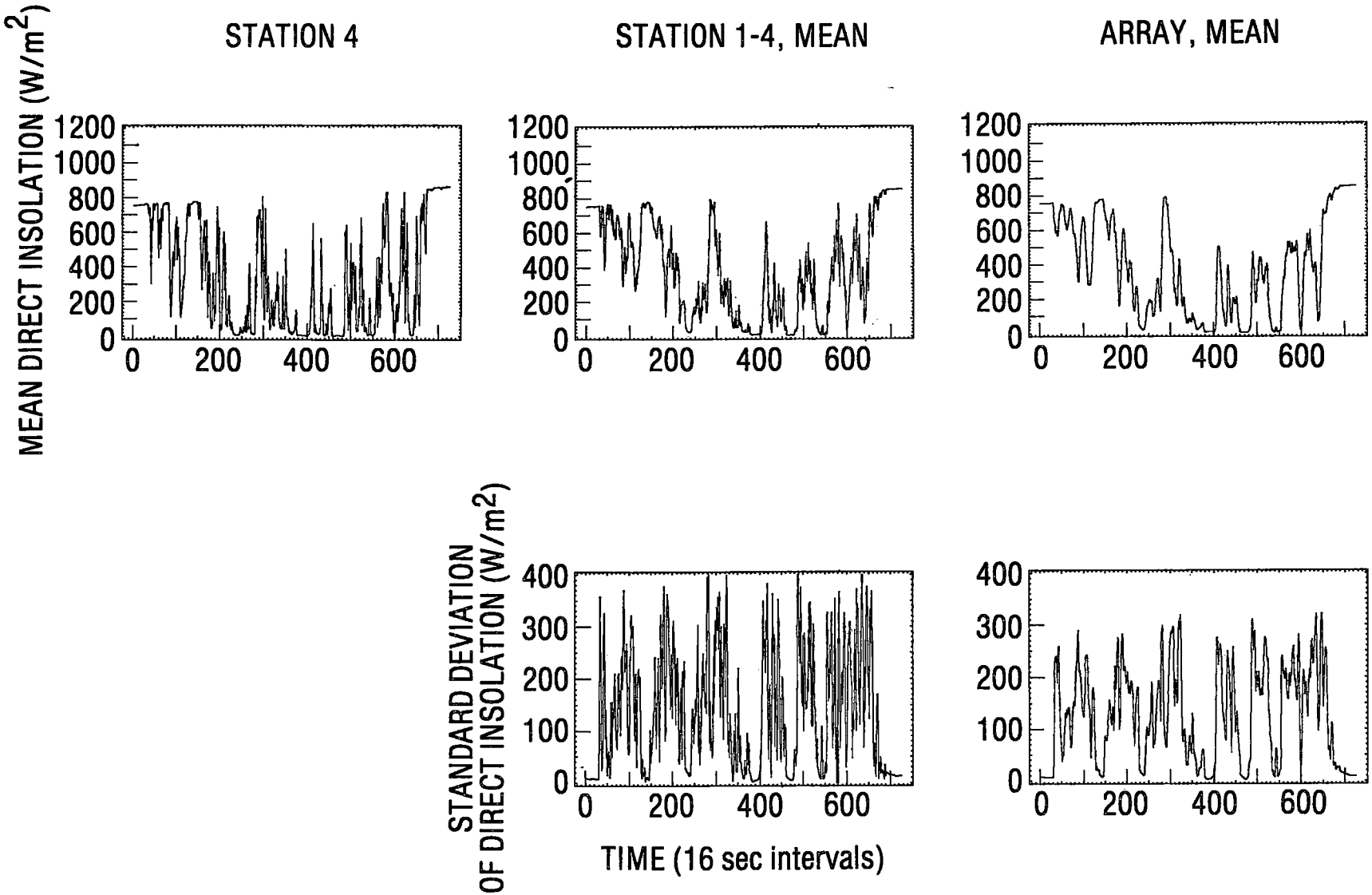

Table 3-4

Persistence of Low Direct Insolation

	Station 4	Station 1-4, Mean	Array Mean
5 August 1978			
No. OF CASES	8	4	3
Duration (sec)			
Minimum	32	64	192
Maximum	2190	2300	2300
Mean	460	800	1070
Standard Dev	738	1050	1100
8 August 1978			
No. OF CASES	35	30	15
Duration (sec)			
Minimum	16	16	16
Maximum	944	1220	1310
Mean	177	165	320
Standard Dev	249	275	396
11 August 1978			
No. OF CASES	18	9	7
Duration (sec)			
Minimum	16	16	80
Maximum	240	304	288
Mean	96	116	169
Standard Dev	71	97	78
26 August 1978			
No. OF CASES	11	3	1
Duration (sec)			
Minimum	16	16	32
Maximum	80	48	32
Mean	26	27	32
Standard Dev	19	19	0

IV. CONCLUSIONS AND RECOMMENDATIONS

A. CONCLUSIONS

On the basis of the initial data analyses presented in this report we summarize here the pertinent information which we believe must be considered in the design for the pilot plant.

1. Clouds will affect the insolation a significant fraction of the time (10-15%) even at a desert location such as Barstow.

2. Shadow dimensions smaller than the collector field have been observed, and dimensions range upwards. A semi-infinite cloud edge crossing the collector array is an inadequate model to describe all aspects of real shadows.

3. A single sensor gives an incomplete description of the insolation variation from the collector field.

4. Rates of insolation change greater than 30 Wm^{-2} sec^{-1} have been observed from a single sensor. This observation may be limited by the 16 sec temporal resolution of the present experiment.

5. The spatial averaging inherent in the several heliostats focused on a single receiver panel reduces the maximum rate of insolation change.

6. The spatial averaging tends to decrease the number of separate outages, but increase the typical length of an outage.

B. RECOMMENDATIONS

On the basis of initial data analyses presented here and informal discussion of these results with representatives of several interested organizations we recommend the following:

1. These data should be considered in the design of the pilot plant, particularly in the design of control systems and the formulation of plant operation strategy.

2. The experiment should be continued to provide data from at least a year and preferably a longer time. This will include data from seasons other than late summer and fall.

3. The experiment should be modified in several ways, each relatively inexpensive, to enhance the applicability of the experiment results to the pilot plant. We recommend the following specific modifications:

   a. Photographs should be taken of sky around the sun before and during partly cloudy events. These photographs will have several uses:

      i. They will provide information to relate variations over the collector field interior to the present insolation sensors.

      ii. They will provide an independent means of determining cloud shadow velocity.

      iii. They will provide positive identification of cloud types for correlation of insolation variation patterns with long term weather records.

      iv. They will provide information about the visual precursors of partly cloudy events for use in planning plant operation strategies.

b. The experiment should be augmented to measure directly peak rates of insolation change and to record these in the data stream.

c. The time resolution of the data taking loop should be increased by decreasing the sampling interval from the current 16 sec value, at least during partly cloudy events.

4. The analysis of data from this experiment must continue, and shift emphasis from a preliminary sampling to a routine approach designed to provided additional information directly related to pilot plant design. This should include the following:

a. Determine the frequency of partly cloudy and overcast events.

b. Characterize the insolation falling on those heliostats feeding a single panel of the receiver.

c. Develop methodology to characterize insolation variation on a regular grid of points over the collector field and apply to derive a quantitative description of insolation variation over the collector field during a typical partly cloudy event.

We believe the information presently available from this experiment is important for the design of the pilot plant, particularly in the area of control systems, and we believe the continued experiment, enhanced as recommended here, will provide important additional quantitative insight into the nature of the insolation resource the Solar Thermal Pilot Plant is designed to tap.

REFERENCES

1. K. L. Zondervan, K. F. Steffan and T. J. Connor, "Dynamic Computer Simulation of the DOE 10 MW Solar Thermal Pilot Plant", AIAA/ASERC Conference on Solar Energy: Technology Status Paper 78-1752, Phoenix, Arizona, 27-29 November 1978.

2. C. M. Randall, M. E. Whitson, J. V. Coggi, "Pilot Plant Environmental Conditions (OPDD Appendix C)", Aerospace Report ATR-78(7695-05)-05, 15 August 1978.

3. N. W. Patapoff, "The West Associates Solar Resource Evaluation Project-Solar Energy Measurements During 1976", Southern California Edison Co., June 1977.

4. R. J. Yinger, "The West Associates Solar Resource Evaluation Project-Solar Energy Measurements at Selected Sites Throughout the Southwest During 1977", Southern California Edison Co., 1978.

5. C. M. Randall, "Barstow Insolation and Meteorological Data Base", Aerospace Corporation Report ATR-78(7695-05)-2, 13 March 1978. Since publication of this report discussing 1976 data, 1977 data has also been prepared in this same format and the entire data set has also been made available in an hourly format.

6. D. B. McKenney, W. T. Beauchamp, "Solar Microclimatology", Helio Associates Report NASA-CR-148533, November 1975.

7. R. T. Hall, "Cloud Shadow Modelling", Section III.A.4 in "Solar Thermal Conversion Mission Analysis, Quarterly Highlights Report", Aerospace Report ATR-75(7506-01), 30 April 1975.

8. R. H. Blackmer and S. M. Serebreny, "Dimensions and Distributions of Cumulus Clouds as Shown by U-2 Photographs", Stanford Research Institute Scientific Report 4, July 1962, AFCRL-62-609.

9. I. A. Lund and M. D. Shanklin, "Universal Methods for Estimating Probabilities of Cloud-Free Lines-of-Sight through the Atmosphere", J. Appl. Meteor. 12, 28-35 (1973).

10. V. G. Planck, "The size distribution of Cumulus Clouds in Representative Florida Populations", J. Appl. Meteor. 8, 46-67 (1969).

11. C. L. Laurence and P. J. Peters, "Solar Collector Transient Studies", Aerospace Report ATR-77(7506-03)-1-R, 4 January 1977.

12. M. D. Gifford, "Characteristic Size Spectra of Cumulus Fields Observed from Satellites", Thesis, Colorado State University/Air Force Institute of Technology, AFTI/CI Report AFIT-CI-78-28, November 1977.

13. G. A. Marotz and J. A. Henry, "Satellite-Derived Cumulus Cloud Statistics for Western Kansas", J. Appl. Meteor. 17, 1725-1736 (1978).

14. E. Flowers, NOAA/ERL Private Communication.

15. E. Flowers, "NOAA Calibration Center", DOE Resource Assessment Branch Review, Manassas, Virginia, 13-16 November 1978.

16. C. M. Randall, "Insolation Data Base Available from The Aerospace Corporation", Aerospace Corporation Report ATR-76(7523-11)-9, December 1976.

17. A brief discussion of the correlation coefficient is given by: A. A. Clifford in "Multivariate Error Analysis" Applied Science Publishers Ltd., London, 1973.

APPENDIX A.

ANALOG TO FREQUENCY SIGNAL CONDITIONING

The solar radiation sensors employed in this experiment have outputs in the millivolt or 0.1 milliamp range. To reliably transmit the information from the sensor to the base station, a signal conditioning circuit was placed close to each sensor. This circuit produced a series of pulses on a balanced output line, at a frequency linearly dependent on the input current or voltage. A block diagram of the system for one channel is shown in Fig. A-1. The base station portion of the system consisting of the line receivers and power supplies for all channels is assembled on a single chassis. The design is straightforward, and further details are not provided here.

The circuit for the voltage to frequency converter is shown in Fig. A-2. This circuit is used with all the Eppley instruments. The circuit used with the Lambda instruments, which electrically are current generators, is shown in Fig. A-3. There is a high degree of commonality between the circuits. The parts list for both circuits is provided by Table A-1. The circuits are assembled on circuit boards about 5" x 4" mounted perpendicularly to a 6" x 6" metal plate. The regulators are mounted on the metal plate for heat sink purposes. The metal plate then becomes the cover for a 6" x 6" x 6" electrical "pull box" which provides protection for the circuit board and connections. At each remote station the pull box is in turn mounted in a meteorological instrument shelter to provide weather protection. For base station instruments the circuits are simply mounted inside the trailer.

Each circuit was calibrated in the laboratory and found to be linear to well within 1% of full scale input. Each circuit was tested at 4 temperatures between $-20^{o}C$ and $+60^{o}C$. The transfer constant (Hz/A, or Hz/V) was found to vary by less than 1% over

FIGURE A-1. **Signal Conditioning Electronics**

BLOCK DIAGRAM

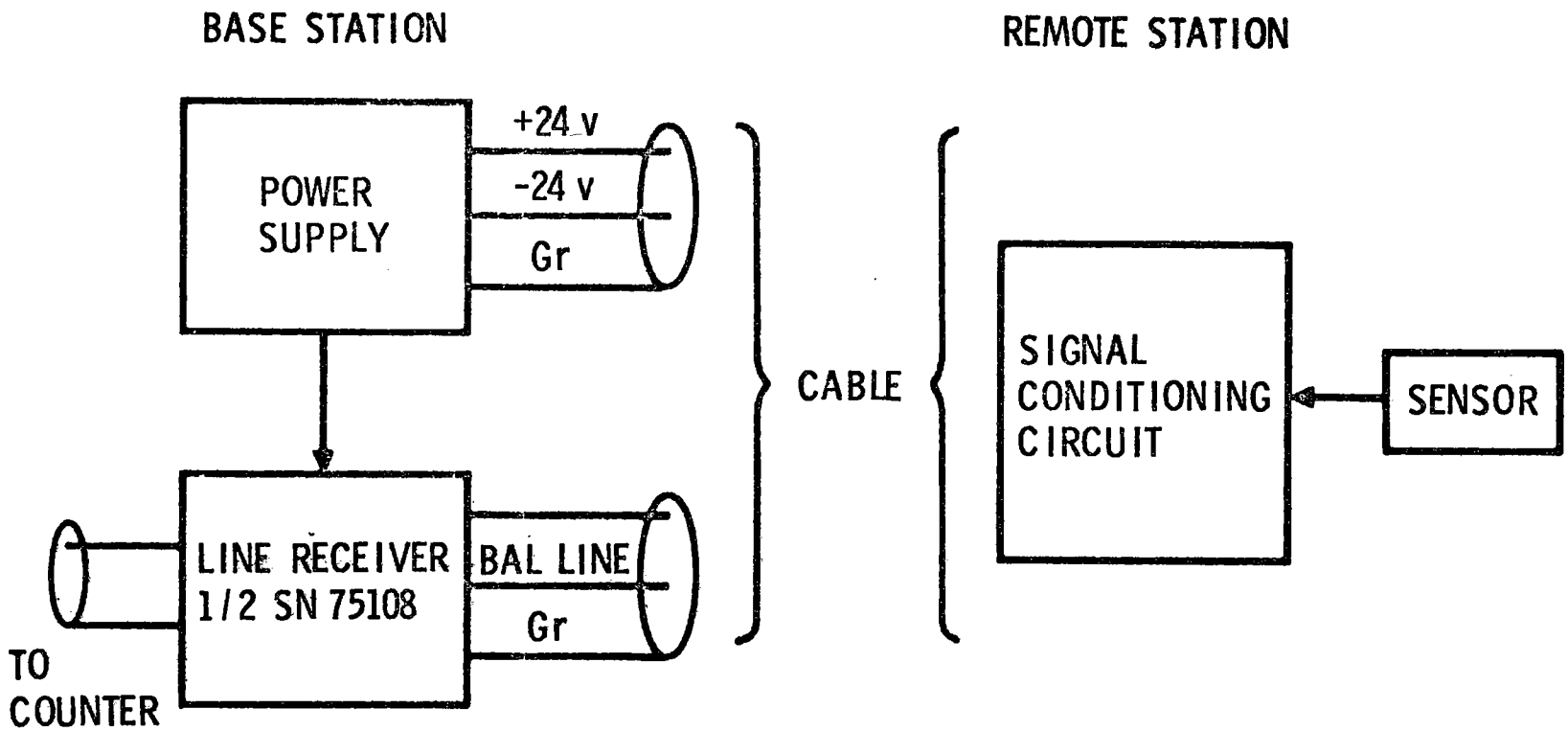

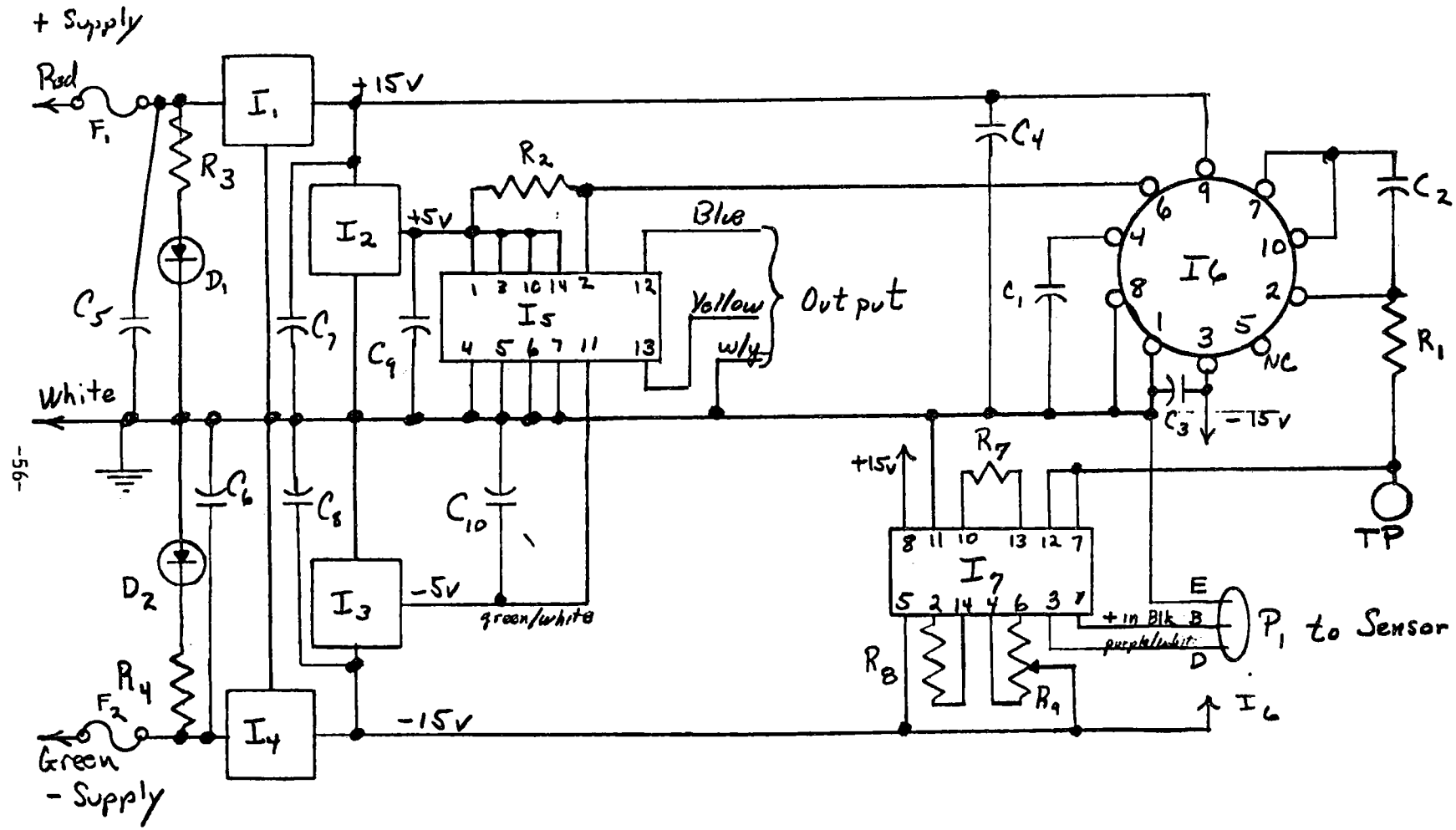

Figure A-2. Voltage to Frequency Converter Schematic Diagram.

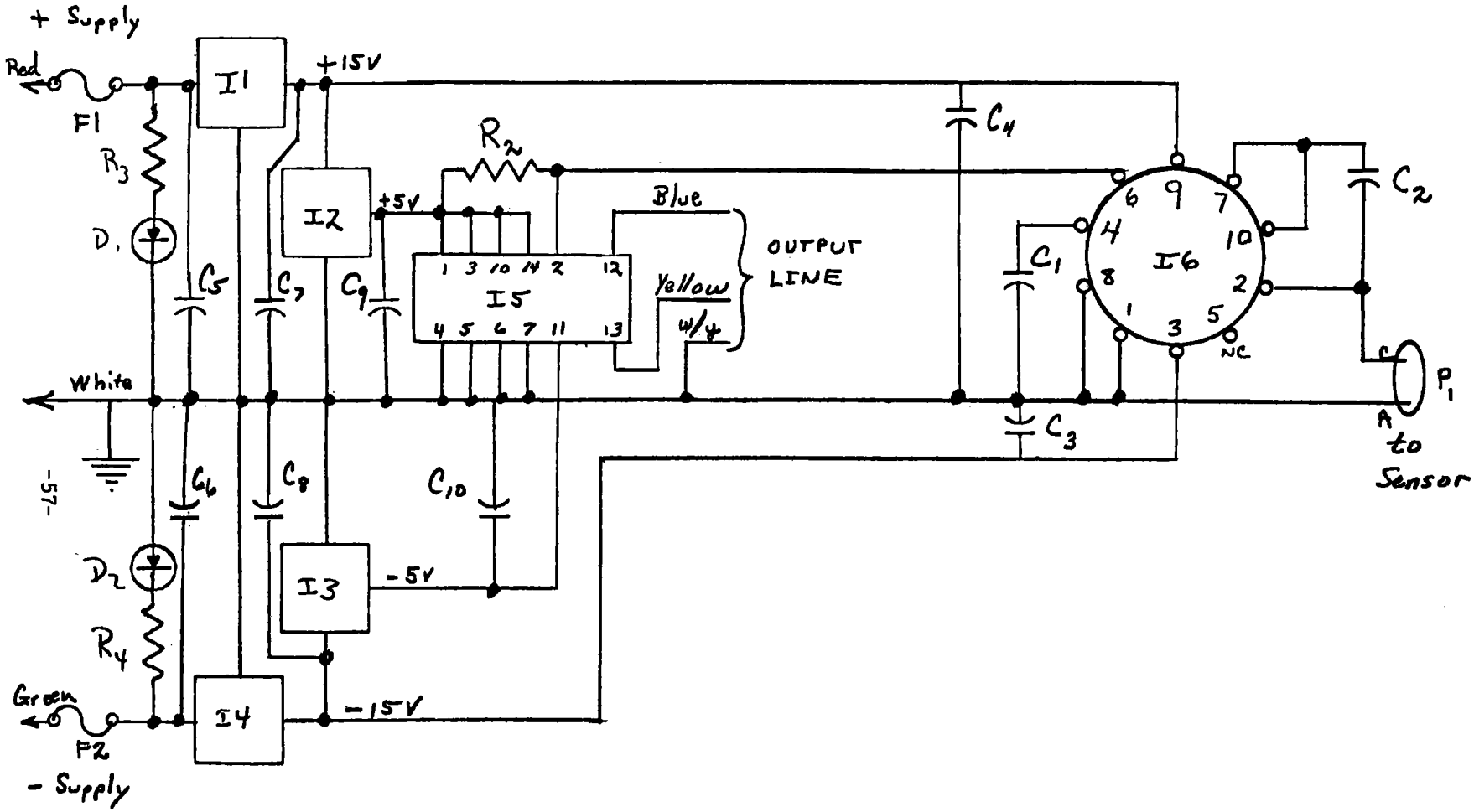

Figure A-3. Current to Frequency Converter Schematic Diagram.

Table A-1. Parts for A/F Converter

Component	Voltage to Frequency	Current to Frequency
R_1	4.02 kΩ, 1%	-
R_3, R_4	2.2 kΩ, 5%	*
R_7	100 kΩ, 1%	-
R_8	1.0 kΩ, 1%	-
R_9	10 kΩ, potentiometer	-
C_1	3300 pfd mica	1320 pfd mica
C_2	0.01 μfd mica	2000 pfd mica
C_3, C_4	0.01 μfd ceramic	*
C_5, C_6	3.3 μfd, 50V	*
C_7, C_8	10 μfd, 20V	*
C_9, C_{10}	33 μfd 10V	*
I_1	+ 15 V regulator, Fairchild A 7815	*
I_2	+ 5 V regulator Fairchild A 7805	*
I_3	- 5 V regulator Fairchild A 7905	* *
I_4	- 15 V regulator Fairchild 7915	* *
I_5	Line Driver, SN55110	*
I_6	Current to Frequency Converter Burr Brown VFC 32	*
I_7	Instrumentation Amplifier Analog Devices AD521	-
D_1	Red LED	*
D_2	Green LED	*
F_1, F_2	1/4 amp fuses	*
P_1	Receptacle for sensor cord	

* Current to frequency model uses same component.
\- Current to frequency model does not need this component.

this entire range, and the linearity was also maintained. The current to frequency circuits showed smaller temperature effects than did the voltage to frequency circuits.

The transfer characteristic of each circuit in use has been monitored in the field by temporarily replacing the sensor with a known voltage or current and observing the frequency recorded on the tape. The record of these electrical calibrations is provided in Table A-2. All circuits have stayed well within 1% of the nominal laboratory values, and with the exception of CMR-9 do not appear to be drifting. Due to the drift in that unit, it was removed from the NIP in December 1978.

Table A-2. Transfer Characteristics of A/F Converters

Unit Identification	Nominal Value (Jul 78)	Station/Channel/ Instrument	Percent Observed Difference from Nominal Value 24 Aug	3 Oct	14 Nov	27 Dec
I/F						
CMR-1	98.23 Hz/ A	2/2/Lambda	-0.05	-0.04	not	+.34
CMR-4	95.84 Hz/ A	4/4/Lambda	+0.01	+0.05	measured	+.08
CMR-5	95.34 Hz/ A	3/3/Lambda	-0.05	-0.10	-	+.01
CMR-6	95.49 Hz/ A	1/1/Lambda	-0.08	-0.06	-	+.01
CMR-7	95.75 Hz/ A	Backup	-	-	-	-
CMR-8	95.67 Hz/ A	4/5/Lambda Shade Ring	-0.07	-0.04	-	-.03
V/F						
CMR-2	860.0 Hz/mV	4/6/Eppley 8-48	+0.12	-0.07	+0.08	+.13
CMR-3	959.5 Hz/mV	4/0/Eppley PSP	-	-0.06	-0.06	+.11
CMR-9	922.6 Hz/mV	4/7/Eppley NIP	-0.23	-0.50	-0.82	-.73

*U.S. GOVERNMENT PRINTING OFFICE: 1980-640-189/4190. Region 4.